Cell Reports
Medicine

Article

Biased agonism of GLP-1R and GIPR enhances glucose lowering and weight loss, with dual GLP-1R/GIPR biased agonism yielding greater efficacy

Graphical abstract

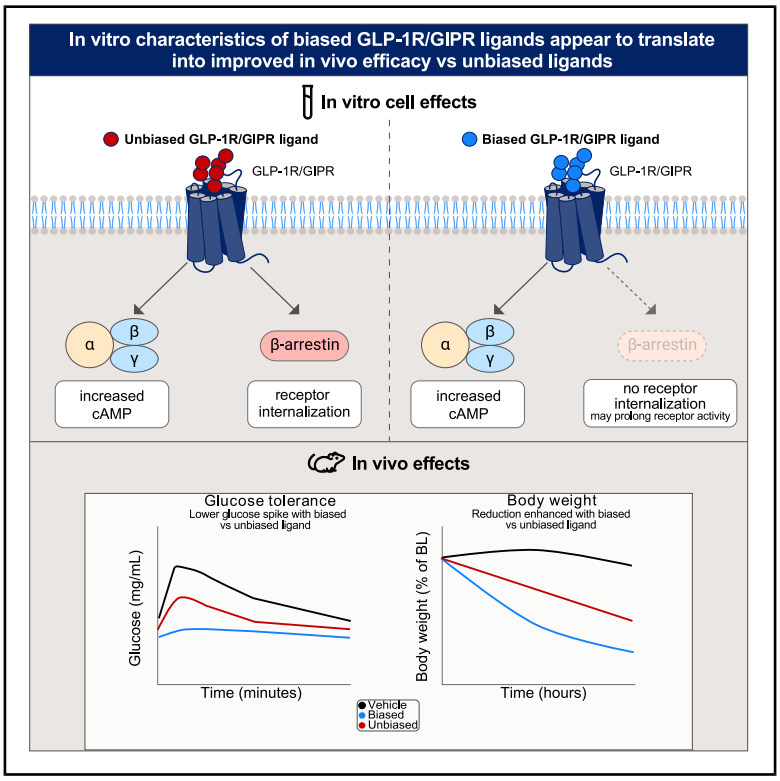

Highlights

- G-protein-biased GLP-1R/GIPR agonists show lower receptor internalization
- Biased agonism of either GLP-1R or GIPR leads to better efficacy on glucose lowering
- Biased agonism of GLP-1R and GIPR leads to greater food intake reduction and weight loss
- Combined agonism of the two receptors synergize on food intake reduction and weight loss

Authors

Ruben Rodriguez, Anne Hergarden, Shyam Krishnan, ..., Stig K. Hansen, Jian Luo, Manu V. Chakravarthy

Correspondence

luo.jian@gene.com (J.L.), chakram5@gene.com (M.V.C.)

In brief

Rodriguez et al. investigate the impact of biased signaling with a dual GLP-1R/GIPR agonist. Biased GLP-1R and GIPR agonism leads to better and prolonged glucose lowering, greater food intake reduction, and weight loss than unbiased agonism. Biased GIPR agonism synergizes with GLP-1R on food intake suppression and weight loss.

Rodriguez et al., 2025, Cell Reports Medicine 6, 102156
June 17, 2025
https://doi.org/10.1016/j.xcrm.2025.102156

CellPress

Cell Reports Medicine

CellPress
OPEN ACCESS

Article

Biased agonism of GLP-1R and GIPR enhances glucose lowering and weight loss, with dual GLP-1R/GIPR biased agonism yielding greater efficacy

Ruben Rodriguez,[1,2] Anne Hergarden,[1,2] Shyam Krishnan,[1] Marikris Morales,[1] Davina Lam,[1] Ted Tracy,[1] Teresa Tang,[1] Avalon Patton,[1] Craig Lee,[1] Asmita Pant,[1] Daniel A. Erlanson,[1] Johan Enquist,[1] Derek Bone,[1] Ray Fucini,[1] Damian Bialonczyk,[1] Stig K. Hansen,[1] Jian Luo,[1,*] and Manu V. Chakravarthy[1,3,*]

[1]Carmot Therapeutics, Berkeley, CA, USA
[2]These authors contributed equally
[3]Lead contact
*Correspondence: luo.jian@gene.com (J.L.), chakram5@gene.com (M.V.C.)
https://doi.org/10.1016/j.xcrm.2025.102156

SUMMARY

Glucagon-like peptide-1 receptor (GLP-1R) and glucose-dependent insulinotropic polypeptide receptor (GIPR) agonists have recently been shown to play a significant role in the treatment of diabetes and obesity. Better understanding of their signaling and mechanism of action could further improve their therapeutic effects. In the current study, we investigate the impact of biased cyclic AMP (cAMP) signaling of GLP-1R and GIPR, individually, as well as the combined effects of a unimolecular dually biased GLP-1R/GIPR agonist, CT-859, on glucose, food consumption, and body weight regulation. Our data demonstrate that biased agonism of either GLP-1R or GIPR leads to better glycemic regulation, greater food intake suppression, and weight loss. In addition, concerted biased activation of both GLP-1R and GIPR results in substantially higher efficacy. Activation of GLP-1R and GIPR with a combination of individually biased agonists or via a dually biased unimolecular approach with CT-859 may provide significant therapeutic advantages for the treatment of diabetes and obesity.

INTRODUCTION

In the United States, the prevalence of obesity among adults has increased from 13% in 1960 to over 40% by 2017, paralleling a significant rise in the prevalence of type 2 diabetes (T2D).[1,2] In response, the biopharmaceutical and medical communities have dedicated significant efforts to developing therapies that simultaneously lower blood glucose (BG) and body weight. Following the 2005 Food and Drug Administration approval of exenatide for glycemic control in T2D, several glucagon-like peptide-1 receptor agonists (GLP-1RAs), such as liraglutide, dulaglutide, and semaglutide, have been introduced. These medications have significantly contributed to the management of BG levels in patients with T2D. Furthermore, at higher doses, liraglutide and semaglutide received approval for weight management in 2014 and 2021, respectively, marking a significant milestone in establishing the role of GLP-1RAs in the treatment of T2D and obesity.[3–6]

In response to meal ingestion, glucagon-like peptide-1 (GLP-1) and glucose-dependent insulinotropic polypeptide (GIP) are released by intestinal L and K cells,[7–11] respectively. In a concerted effort, they effectively regulate postprandial glycemia, energy consumption, and metabolism.[12] Based on this premise, tirzepatide, a dual GIP receptor (GIPR)/GLP-1 receptor (GLP-1R) agonist, was developed.[13] In clinical studies, tirzepatide showed unprecedented efficacy for glucose lowering and weight loss in patients with T2D, as well as achieved superior weight loss in patients with obesity compared to GLP-1R mono-agonists (e.g., semaglutide).[14,15] Interestingly, *in vitro* studies indicate that tirzepatide mimics the actions of native GIP at its receptor but exhibits unique signaling properties at GLP-1R. At GLP-1R, tirzepatide favors cyclic AMP (cAMP) accumulation over β-arrestin recruitment and is less effective at inducing receptor internalization than the native ligand.[16] This biased signaling may lead to the retention of GLP-1R at the plasma membrane, generating greater efficacy. Indeed, a great body of work has demonstrated that biased GLP-1RAs elicit better glycemic benefits compared to their "unbiased" counterparts, though the impact on weight loss is less certain.[17–22] Therefore, the increased efficacy of tirzepatide may be attributed to multiple factors, while the exact mechanisms remain to be better understood. Adding to the complexity, tirzepatide is much less potent at the mouseGIPR than the humanGIPR, which limits the use of rodent models for mechanism-of-action studies.[23]

The lack of β-arrestins recruitment is advantageous for glucose reduction and weight loss associated with GLP-1R agonists. The function of β-arrestin recruitment at the GIPR remains less defined. Research has indicated that the absence of β-arrestin-2 diminishes glucose-stimulated insulin secretion in isolated mouse islets in response to GIP.[24] Furthermore, another

study found that mice deficient in β-arrestin-2 do not respond to d-Ala GIP during an intraperitoneal glucose tolerance test (ipGTT).[25] However, investigations in INS-1 832/3 cells have also demonstrated that a GIPR agonist that does not recruit β-arrestin enhances insulin secretion more than GIP.[26] In a separate study involving a β cell-specific β-arrestin-2 knockout, Bitsi et al. reported that in response to D-ala2-GIP, mice lacking β-arrestin-2 in β cells tended to maintain lower glucose levels during a glucose tolerance test.[27] The discrepancies among these studies highlight the complexities of β-arrestin signaling at the GIPR.

Recognizing that concerted activation of the GLP-1R and GIPR may lead to better efficacy and that biased signaling toward cAMP generation may further enhance it, we used chemotype evolution, a method that provides rapid access to large chemical diversity, to discover and engineer CT-859, a dual GLP-1R/GIPR agonist with biased signaling toward cAMP generation for both receptors (Figure S1). Chemotype evolution starts with a designed "bait" compound that is selected based on information about the target. The bait contains a reactive functionality that can be linked to molecules from a collection of fragments. The resulting custom library of chimeric molecules is screened against the target in cAMP and β-arrestin plate-based assays with one compound per well format. CT-859 was identified from this screen and found to stimulate cAMP generation at both the GLP-1R and GIPR. CT-859 also lacked β-arrestin recruitment at both receptors. We chose to characterize CT-859 in this study because it has similar signaling properties at mouse receptors as CT-868 has at human receptors, a once daily dual-biased GLP-1R/GIPR agonist currently in phase 2 clinical trials. We chose liraglutide as a comparator because it is an unbiased GLP-1RA that is also dosed clinically once daily. Furthermore, we developed other tool compounds (biased and unbiased GIPR agonists) to substantiate our efficacy observations and, crucially, to delineate the role of each receptor and the importance of biased signaling on glycemic control, energy consumption, and weight loss.

Our data demonstrate that biased signaling toward cAMP with limited β-arrestin recruitment prevented receptor internalization for both the GLP-1R and GIPR. Treatment with CT-859 led to greater and much-prolonged glucose reduction in mice compared to that of liraglutide. More importantly, food intake reduction and weight loss following sub-chronic treatment with CT-859 were also superior to liraglutide. Studies in GLP-1R or GIPR knockout mice provided insights into the synergistic role of activating both GLP-1R and GIPR in a bifunctional molecule. Furthermore, by leveraging tool molecules of GIPR agonists, we established a role of biased GIPR activation in glycemic homeostasis, food consumption, and weight loss. Like GLP-1R, there are centrally mediated effects of GIPR activation on energy consumption and weight loss, and greater efficacy can be achieved through concerted biased activation of both receptors. The findings of these studies substantiate the notion that biased activation, not just of GLP-1R but also of GIPR, enhances efficacy, and dual-biased activation of GLP-1R/GIPR may be therapeutically superior for the treatment of T2D and obesity.

RESULTS

CT-859 is a biased dual GLP-1R/GIPR agonist and does not induce receptor internalization

Utilizing recombinant cell lines expressing GLP-1R or GIPR, *in vitro* activities of CT-859 were characterized by cAMP accumulation, β-arrestin coupling, and receptor internalization. CT-859 is a full agonist for cAMP accumulation at mouse GLP-1R and is 113 times less potent than native ligand GLP-1 and 12 times less potent than liraglutide (EC_{50}: GLP-1 3 pM, liraglutide 29 pM, and CT-859 343 pM, Figure 1A). However, CT-859 exhibits modality bias, as it elicits negligible (<5%) recruitment of either β-arrestin-2 or β-arrestin-1 to mouse GLP-1R vs. GLP-1 (99% or 122%) and liraglutide (98% or 122%) (Figure 1B; Table S1). At mouse GIPR, CT-859 is a partial agonist (44% E_{max}) for cAMP accumulation, with 48 times lower potency than GIP to drive cAMP accumulation (1.6 vs. 32 pM respectively, Figure 1F). Similar to the effects at GLP-1R, CT-859 also has negligible (<5%) recruitment of β-arrestin-2 to mouse GIPR vs. GIP (Figure 1G). Since limited interaction has been reported between GIPR and β-arrestin-1,[28] this interaction was not assessed. Next, we investigated the effects on receptor internalization. In contrast to GLP-1 and liraglutide, which drive human GLP-1R internalization with EC_{50} values of 1.7 and 10.2 nM and E_{max} values of 56% and 75%, respectively, CT-859 did not cause receptor internalization (E_{max} −16%; Figures 1C and 1D). To the contrary, 2-h exposure to CT-859 increased GLP-1R surface expression compared to vehicle-treated cells (Figure 1D). CT-859 had a similar effect at human GIPR, stimulating greater surface expression than vehicle (Figures 1H and 1I). This implies that CT-859 acts as an antagonist of β-arrestin coupling. Indeed, CT-859 inhibited the native ligand-mediated recruitment of β-arrestin-2 at the GLP-1R and GIPR (Figures 1E and 1J). These incretin receptors are highly conserved across species; human and mouse GLP-1R are 92% identical and 94% similar, while human and mouse GIPR are 81% identical and 85% similar. As ligand cAMP and β-arrestin coupling properties are similar at both receptors (Table S1) and given that GIPR internalization is β-arrestin dependent,[29] we anticipate that similar trends would be observed for human and mouse receptors. Despite a report that mouse GIPR recruits β-arrestin-2 and internalizes more weakly than human GIPR,[30] we are clearly able to measure β-arrestin-2 recruitment and internalization of mouse GIPR (Figure 1G; Tables S1 and S2). We sought to demonstrate that CT-859 is cAMP biased at both receptors. However, future studies are warranted in order to gain a deeper understanding into the role of β-arrestin on receptor signaling, the role of internalization and surface expression on signaling, and the possibility that CT-859 exhibits G protein bias. Of note, there was no observed off-target activity at the mouse glucagon receptor, as 1 μM CT-859 had less than 20% cAMP activity, whereas glucagon had 17 nM EC50.

CT-859 improves glucose levels primarily through GLP-1R activation at lower doses

We first characterized the glucose-lowering effects of CT-859 in lean C57BL/6J mice. CT-859 lowered glucose levels during

CellPress
OPEN ACCESS

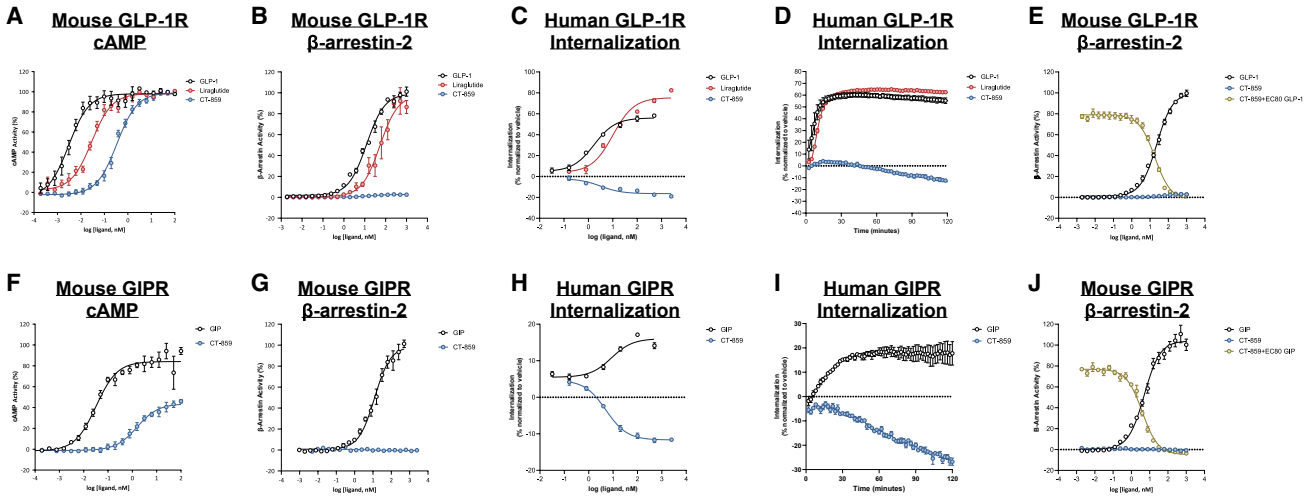

Figure 1. CT-859 is a biased dual GLP-1R/GIPR agonist

(A–E) Mean (±SE, n = 3–4 replicates) (A) cAMP accumulation and (B) β-arrestin-2 coupling at the GLP-1R, (C) GLP-1R internalization, (D) time course for GLP-1R internalization at 100 nM after GLP-1, liraglutide, and CT-859, and (E) inhibition of GLP-1-mediated β-arrestin-2 coupling by CT-859 at the GLP-1R.

(F–J) (F) cAMP accumulation and (G) β-arrestin-2 coupling at the GIPR, (H) GIPR internalization and (I) time course for GIPR internalization at 100 nM after GIP and CT-859, and (J) inhibition of GIP-mediated β-arrestin-2 coupling by CT-859 at the GIPR. Nonlinear regression analysis with the Hillslope constrained to 1 was used to fit normalized *in vitro* data to a curve. Compound potency (EC_{50}) and efficacy (E_{max}) were extracted from this analysis.

an ipGTT 4 h post treatment administration, with an ED_{50} of 0.46 nmol/kg (Figures S2A and S2B), whereas liraglutide had an ED_{50} of 7.3 nmol/kg in the same setting (Figures S2C and S1D). We next assessed how each receptor (GLP-1R and GIPR) contributes to the glucose-lowering effects of CT-859 by conducting ipGTTs in GLP-1R$^{-/-}$ mice, GIPR$^{-/-}$ mice, and their wild-type ($^{+/+}$) littermates (see validation of these mice in Figures S3A–S3D). In GLP-1R$^{+/+}$ mice, CT-859 effectively lowered glucose levels at both 20 and 200 nmol/kg doses compared to vehicle (Figures S2E and S2G). Conversely, in GLP-1R$^{-/-}$ mice, CT-859 at 20 nmol/kg was ineffective at lowering glucose levels, but a dose of 200 nmol/kg achieved a 46% reduction, in contrast to a 75% reduction in GLP-1R$^{+/+}$ mice at the same dose (Figures S2F and S2G). This indicates that the glucose-lowering effect at 20 nmol/kg was mainly mediated through GLP-1R, while at 200 nmol/kg, GIPR was likely involved. In GIPR$^{-/-}$ mice, both doses of CT-859 (20 and 200 nmol/kg) were efficacious at lowering glucose levels. Compared to GIPR$^{+/+}$, the glucose improvement with 20 nmol/kg of CT-859 was maintained in GIPR$^{-/-}$ mice (Figures S2H–S2J). These results indicate that the glucose-lowering effects of CT-859 at 20 nmol/kg are dominated by GLP-1R activation and do not require the engagement of GIPR; we will henceforth term this dose a "non-GIPR-engaging dose." To further confirm that the 200 nmol/kg dose is engaging GIPR and not having an off-target effect, we tested this dose in GLP-1R$^{-/-}$ mice in the presence of the GIPR antagonist and conducted an ipGTT. The glucose improvement induced by CT-859 was completely reversed by compound 7,[31] a GIPR antagonist (Figures S2K and S2L). These results demonstrate that at a higher dose, CT-859 engages both GLP-1R and GIPR specifically in enhancing glucose regulation.

At a non-GIPR-engaging dose, CT-859 demonstrated a prolonged glucose-lowering effect compared to liraglutide

To assess whether there is a difference in glucose-lowering effects between biased and unbiased GLP-1R agonism, we performed ipGTTs in GIPR$^{-/-}$ mice using 20 nmol/kg, a non-GIPR-engaging dose, and compared it to an equal molar dose of liraglutide. CT-859 and liraglutide effectively lowered glucose levels 4 h following a single dose (Figures 2A and 2D). However, liraglutide no longer differed from vehicle 24 h after treatment, while CT-859 maintained its activity at 24 and 48 h (Figures 2B–2D). Similar studies were conducted in lean C57BL/6J mice and diet-induced obese (DIO) mice. Consistent with the results in GIPR$^{-/-}$ mice, we found that CT-859 remained efficacious up to 48 h post drug administration, whereas liraglutide was no longer different from vehicle in both lean C57BL/6J and DIO mice (Figures 2E–2L). However, in contrast to GIPR$^{-/-}$ and lean mice, CT-859 was more efficacious than liraglutide at 4 h in DIO mice (Figures 2I and 2L). To exclude the possibility that prolonged glucose lowering is due to differences in drug exposure, we compared the pharmacokinetics of CT-859 and liraglutide in mice. In a pharmacokinetics study, CT-859 had a longer half-life, but liraglutide had 6 times more exposure than CT-859 (Figure S4A). In a separate study, liraglutide had greater exposure after 14 days of daily dosing in DIO mice (Figure S4B). These data support that the observed difference in glucose lowering is intrinsic to CT-859 and may be the result of its biased signaling at the GLP-1R. To further substantiate our findings, we employed Exendin-Phe1 (Ex-Phe1), a cAMP-biased agonist that prevents receptor internalization (Figures S5A–S5D). In an ipGTT conducted 8 h post drug administration, a single dose of Ex-Phe-1 demonstrated sustained efficacy,

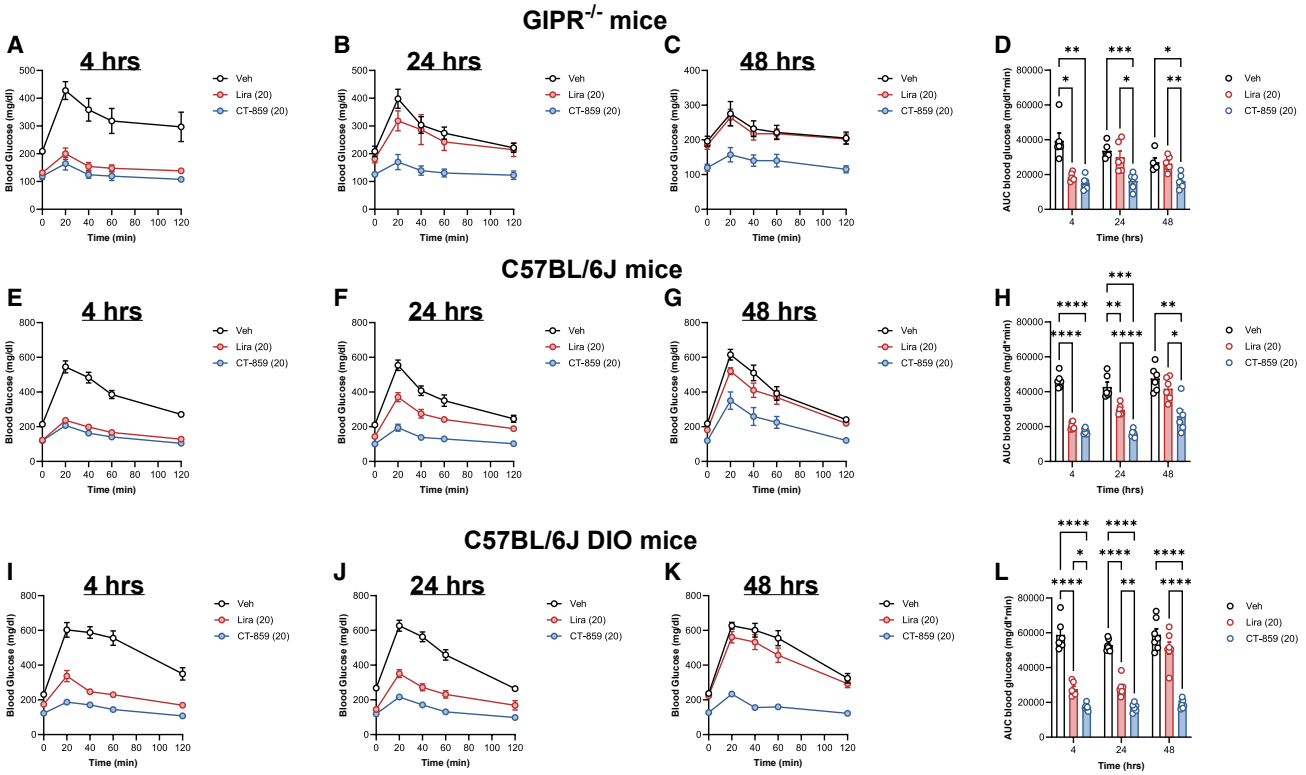

Figure 2. Biased GLP-1R agonists lower glucose over a longer duration than unbiased GLP-1R agonists

Mean (±SE) glucose response to an ipGTT in GIPR$^{-/-}$ mice (A) 4 h, (B) 24 h, and (C) 48 h after vehicle ($n = 5$–6), liraglutide (20 nmol/kg; $n = 6$), and CT-859 (20 nmol/kg; $n = 6$) administration and (D) the area under the glucose curves. Glucose response to an ipGTT in lean C57BL/6J mice (E) 4 h, (F) 24 h, and (G) 48 h after vehicle ($n = 6$), liraglutide (20 nmol/kg; $n = 6$), and CT-859 (20 nmol/kg; $n = 6$) administration and (H) the area under the glucose curves. Glucose response to an ipGTT in C57BL/6J-DIO mice (I) 4 h, (J) 24 h, and (K) 48 h after vehicle ($n = 6$–7), liraglutide (20 nmol/kg; $n = 6$–7), and CT-859 (20 nmol/kg; $n = 6$–7) administration and (L) the area under the glucose curves.

Statistical differences were evaluated using a two-way ANOVA followed by Bonferroni post hoc test. *$p < 0.05$, **$p < 0.01$, ***$p < 0.001$, ****$p < 0.0001$.

while the unbiased GLP-1R agonist exendin-4 (Ex-4) had lost its effectiveness (Figures S5E and S5F).

Central administration of CT-859 at a non-GIPR-engaging dose decreases body weight more than liraglutide

Studies have indicated that GLP-1R agonists suppress food intake through a centrally mediated (i.e., brain) mechanism.[32–35] To characterize the central effects of CT-859 on food consumption and weight loss, we administered it directly to the lateral ventricle by intracerebroventricular (ICV) injection. ICV administration is not intended to represent physiological conditions but enables us to understand the action of these ligands on central targets. To delineate how each receptor contributes to the observed effects, we administered CT-859 at 0.3 and 3 nmol in GLP-1R$^{-/-}$ mice and their GLP-1R$^{+/+}$ littermates. Both doses suppressed food consumption and reduced body weight in GLP-1R$^{+/+}$ mice, but only the high dose suppressed food consumption and reduced body weight in GLP-1R$^{-/-}$ mice (Figures 3A and 3B), indicating that CT-859 was likely not engaging GIPR at 0.3 nmol. To ensure no GIPR engagement, we administered a low dose of CT-859 (0.025 nmol). This dose suppressed food consumption and reduced body weight in GLP-1R$^{+/+}$ mice but had no effect in GLP-1R$^{-/-}$ mice (Figures 3C and 3D), suggesting that CT-859's effects on food consumption and body weight at this dose are mediated through activation of GLP-1R without engaging GIPR. Next, to characterize the central effects of biased and unbiased GLP-1R activation on food consumption and weight loss, we administered CT-859 (0.025 nmol) and liraglutide (0.025 nmol) by ICV in lean C57BL/6J mice. Both significantly decreased body weight, but the reduction with CT-859 (−9% vs. vehicle at 24 h) was greater than liraglutide (−4% vs. vehicle at 24 h) (Figure 3E). Consistent with the reduction in body weight, both suppressed food intake overnight, but the reduction with CT-859 (−63% vs. vehicle at 24 h) was significantly greater than with liraglutide (−33% vs. vehicle at 24 h) (Figure 3F). To further substantiate that these differences were mediated by biased signaling at the GLP-1R, we assessed the effects of Ex-Phe1 in lean C57BL/6J mice. ICV administration of both Ex-Phe1 and Ex-4 lowered food intake and body weight (Figures S5G and S5H); however, Ex-4's effects diminished by 48 h, whereas Ex-Phe1 remained efficacious (Figures S5G and S5H). These data are consistent with the notion that acute

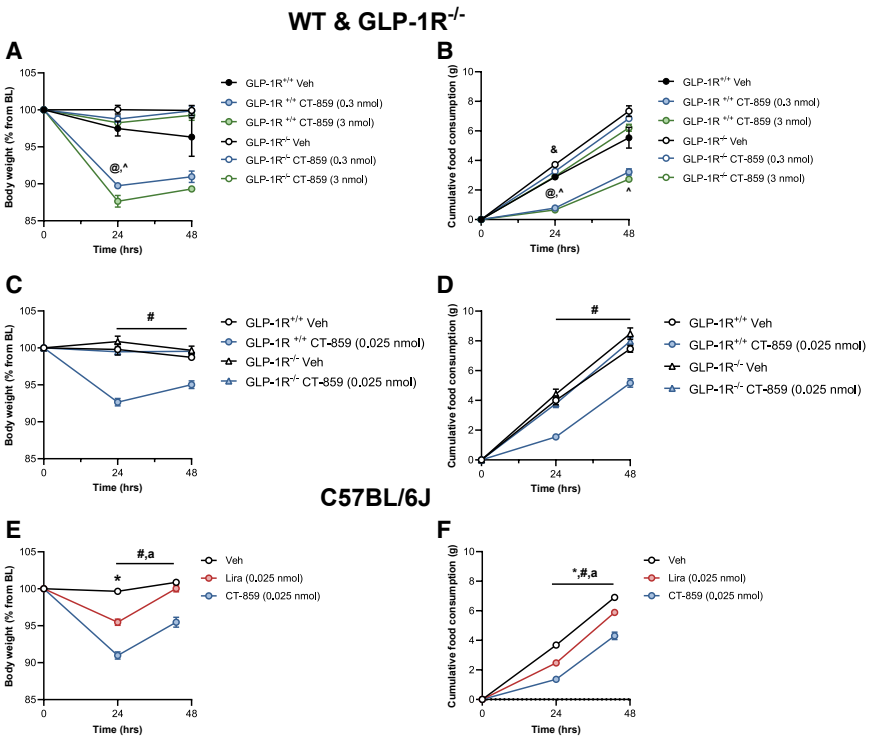

Figure 3. ICV administration of CT-859 decreased food consumption and body weight more than liraglutide

(A and B) Mean (±SE) (A) body weight and (B) cumulative food consumption after ICV administration of vehicle (n = 5) and CT-859 (0.3; n = 5 and 3 nmol; n = 6) in GLP-1R$^{+/+}$ and GLP-1R$^{-/-}$ mice.

(C and D) (C) Body weight and (D) cumulative food consumption after ICV administration of vehicle (n = 6) and CT-859 (0.025 nmol; n = 5–6) in GLP-1R$^{+/+}$ and GLP-1R$^{-/-}$ mice.

(E and F) (E) Body weight and (F) cumulative food consumption after ICV administration of vehicle (n = 9), liraglutide (0.025 nmol; n = 9), and CT-859 (0.025 nmol; n = 5) in lean C57BL/6J mice.

Statistical differences were evaluated using a two-way ANOVA followed by Bonferroni post hoc test. @ = $p < 0.05$; GLP-1R$^{+/+}$ vehicle vs. GLP-1R$^{+/+}$ 0.3 nmol, ^$p < 0.05$; GLP-1R$^{+/+}$ vehicle vs. GLP-1R$^{+/+}$ 3 nmol, & = $p < 0.05$; GLP-1R$^{-/-}$ vehicle vs. GLP-1R$^{-/-}$ 3 nmol; *$p < 0.05$; vehicle vs. liraglutide (0.025 nmol), #$p < 0.05$: vehicle vs. CT-859 (0.025 nmol), a = $p < 0.05$; liraglutide (0.025 nmol) vs. CT-859 (0.025 nmol).

biased agonism of GLP-1R leads to better suppression of food consumption and reduction of body weight.

Sub-chronic administration of CT-859, both at non-GIPR-engaging and GIPR-engaging doses, decreases body weight more than liraglutide

To further assess the difference between a biased and unbiased GLP-1R agonist, we performed chronic studies in DIO mice. Using once daily administration (QD), first, we compared CT-859 at a non-GIPR-engaging dose (20 nmol/kg) to liraglutide (20 nmol/kg). Both CT-859 and liraglutide reduced body weight progressively and initially to a similar extent. However, after a week of dosing, CT-859 started to outperform liraglutide, and by the end of the study, CT-859 had achieved significantly more weight loss (−20% vs. vehicle) than liraglutide (−13% vs. vehicle) (Figure 4A). CT-859 also lowered inguinal adipose (−40% vs. vehicle) whereas liraglutide had no effect (Figure S6A). Both treatments did not affect epididymal adipose (Figure S6B) and similarly lowered liver weights (Figure S6C). Additionally, CT-859 significantly reduced fasting BG (−33% vs. vehicle) and the homeostatic model assessment of insulin resistance (log(HOMA-IR)) (−45% vs. vehicle) compared to liraglutide (−10% and −20% vs. vehicle, respectively) (Figures 4C and 4E). Both CT-859 and liraglutide lowered fasting insulin levels relative to vehicle (Figure 4D). Interestingly, treatment of CT-859 induced less food intake suppression on day 1 and equal food intake suppression on days 7 and 14 compared to liraglutide (Figure 4B), indicating that the weight loss observed with biased GLP-1R activation may involve additional mechanisms. Next, to assess the full efficacy potential of biased GLP-1R/GIPR dual agonism, we administered CT-859 (200 nmol/kg; QD), a GIPR-engaging dose, and liraglutide (200 nmol/kg; QD) for 19 days in DIO mice. Following a similar pattern, both CT-859 and liraglutide initially reduced body weight equally. However, after 3 days of dosing, CT-859 started to outperform liraglutide, and by the end of the study, CT-859 had significantly more weight loss (−33% vs. vehicle) than liraglutide (−22% vs. vehicle) (Figure 4F). Inguinal and epididymal fat masses were also significantly lower with this dose of CT-859 (−71% and −61% vs. vehicle, respectively; Figures S6D and S6E), while liver weights were similarly decreased between treatments (Figure S6F). Moreover, CT-859 lowered fed glucose and insulin levels (−20% and −75% vs. vehicle; respectively), whereas liraglutide had no significant effect (Figures 4H and 4I). Both treatments improved log(HOMA-IR) compared to vehicle (Figure 4J). Like the lower dose, CT-859 suppressed food intake equally to liraglutide on day 1, but notably, CT-859 suppressed food intake (−65% vs. vehicle) significantly more than high-dose liraglutide (−42% vs. vehicle) on day 7 and trended on day 14 (Figure 4G). This suggests that engagement of GIPR may have altered the dynamics of the effects of CT-859 on food intake. To confirm the observation, we compared the high dose (200 nmol/kg) of CT-859 to a caloric restriction group (60% restriction). At this dose, CT-859 decreased body weight more than 60% caloric restriction, even though cumulative food consumption between the groups was equal (Figures S6G and S6H). These results suggest that in addition to decreasing food intake, CT-859 may decrease body weight through other mechanisms.

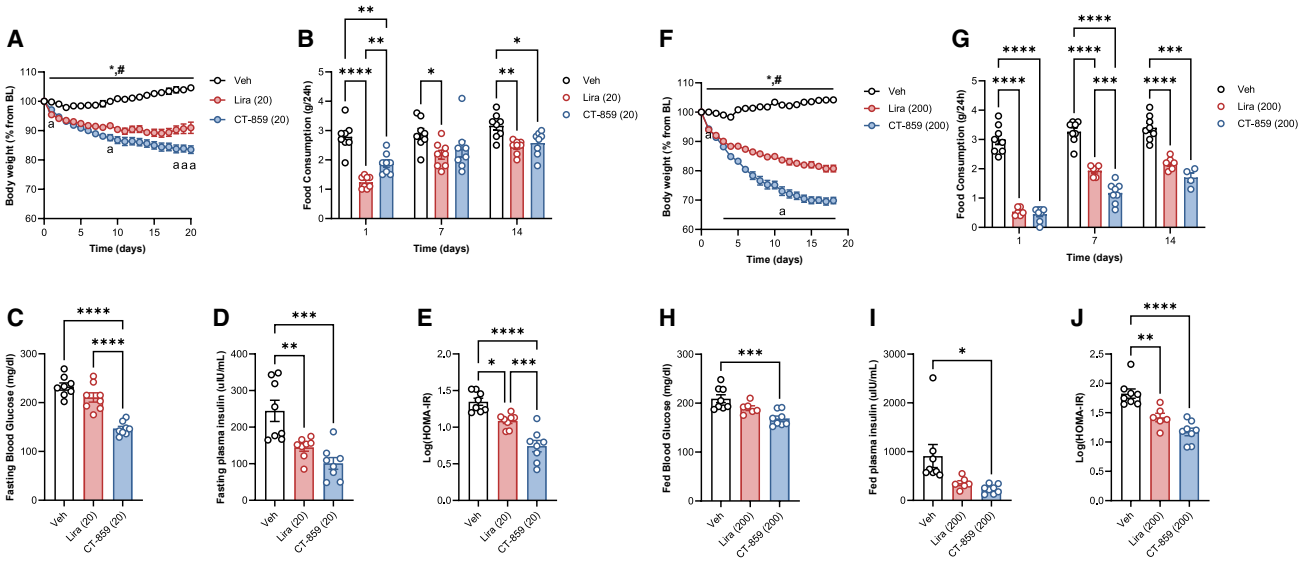

Figure 4. CT-859 decreases body weight more than liraglutide at non-GIPR- and GIPR-engaging doses in DIO mice

(A–E) Mean (±SE) (A) body weight, (B) food consumption, (C) fasting blood glucose, (D) fasting plasma insulin, and (E) log(HOMA-IR) in C57BL/6J DIO mice treated with vehicle (n = 8), liraglutide (20 nmol/kg; n = 8), and CT-859 (20 nmol/kg; n = 8) for 19 days.

(F–J) (F) Body weight, (G) food consumption, (H) fed blood glucose, (I) fed plasma insulin, and (J) log(HOMA-IR) in C57BL/6J DIO mice treated with vehicle (n = 8), liraglutide (200 nmol/kg; n = 6), and CT-859 (200 nmol/kg; n = 8) for 19 days.

Statistical differences were evaluated using a one-way ANOVA or two-way ANOVA followed by Bonferroni post hoc test. *p < 0.05; **p < 0.01, ***p < 0.001; ****p < 0.0001; for (A), *p < 0.05; vehicle vs. liraglutide (20 nmol/kg), #p < 0.05: vehicle vs. CT-859 (20 nmol/kg), a = p < 0.05; liraglutide (20 nmol/kg) vs. CT-859 (20 nmol/kg); for (F), *p < 0.05; vehicle vs. liraglutide (200 nmol/kg), #p < 0.05: vehicle vs. CT-859 (200 nmol/kg), a = p < 0.05; liraglutide (200 nmol/kg) vs. CT-859 (200 nmol/kg).

GIPR activation suppresses food intake and reduces body weight, and a biased GIPR agonist is superior to an unbiased GIPR agonist

The role of GIPR activation in body weight regulation remains debated as there is evidence that both GIPR agonism and antagonism can reduce adiposity and body weight.[36,37] To further understand this, we engineered CT-693, an unbiased GIPR agonist, and CT-666, a biased GIPR agonist. Both CT-693 and CT-666 are potent agonists for cAMP generation at the mouse GIPR (EC_{50} of 14 and 66 pM, respectively; Figure 7A; Table S2). However, CT-693 couples to β-arrestin-2 with 92% efficacy and promotes receptor internalization, whereas CT-666 does not couple to β-arrestin-2 (<5% efficacy) and does not lead to receptor internalization (Figures S7B–S7D; Table S2). As noticed with CT-859, we observe weaker interactions of CT-693 and CT-666 with the mouse GIPR than with the human GIPR, with the efficacy of cAMP accumulation being 82% versus 94% and 74% vs. 92%. The two molecules have a very similar pharmacokinetic profile (T1/2: CT-693 0.443 h and CT-666 0.493 h) (Figure S7I) and lower glucose levels dose-dependently during an ipGTT in mice (Figures S7E–S7H), demonstrating target receptor engagement. A direct comparison of the two molecules showed that CT-666 had longer glucose reduction compared to CT-693 in an ipGTT in mice (Figures 5A–5C). Since the half-lives of these molecules are short following peripheral administration, making it difficult to assess their effects on food intake and body weight, we directly administered CT-693 and CT-666 via ICV to the lateral ventricle. Both CT-693 and CT-666 significantly suppressed food intake and reduced body weight 24 h after the dose. However, CT-666 was much more effective in reducing food consumption (−68% vs. vehicle at 24 h) and body weight (−9% vs. vehicle at 24 h) compared to CT-693 (−24% vs. vehicle at 24 h and −3% vs. vehicle at 24 h, respectively) (Figures 5D and 5E). CT-666 continued to be more effective than CT-693 at the 48-h time point.

Biased GIPR activation synergized with GLP-1R agonism on food intake suppression and weight loss

To further characterize the interaction between GLP-1R and GIPR activation and their pharmacological effects, we employed the central administration model. We activated the GLP-1R with CT-859 at a non-GIPR-engaging dose and subsequently combined it with unbiased and biased GIPR activation using CT-693 and CT-666, respectively. Consistent with the aforementioned data, activation of GLP-1R and GIPR individually suppressed food intake and promoted weight loss, with the biased GIPR agonist showing greater magnitude and prolonged effects compared to the unbiased GIPR agonist (Figures 6A and 6B). When combining CT-859 with CT-693, significantly greater food intake suppression (−72% vs. vehicle at 24 h) and weight loss (−11% vs. vehicle at 24 h) were observed compared to CT-693 alone (food intake: −26% vs. vehicle at 24 h; weight loss: −3% vs. vehicle at 24 h) but not compared to CT-859 alone. When combining CT-859 with CT-666, significantly greater food intake suppression (−85% vs. vehicle at 24 h) and weight loss (−13% vs. vehicle at 24 h) were observed compared to CT-859 and CT-666 individually (food intake: −54%, −45% vs. vehicle at 24 h, respectively; weight loss: −9%, −6% vs. vehicle

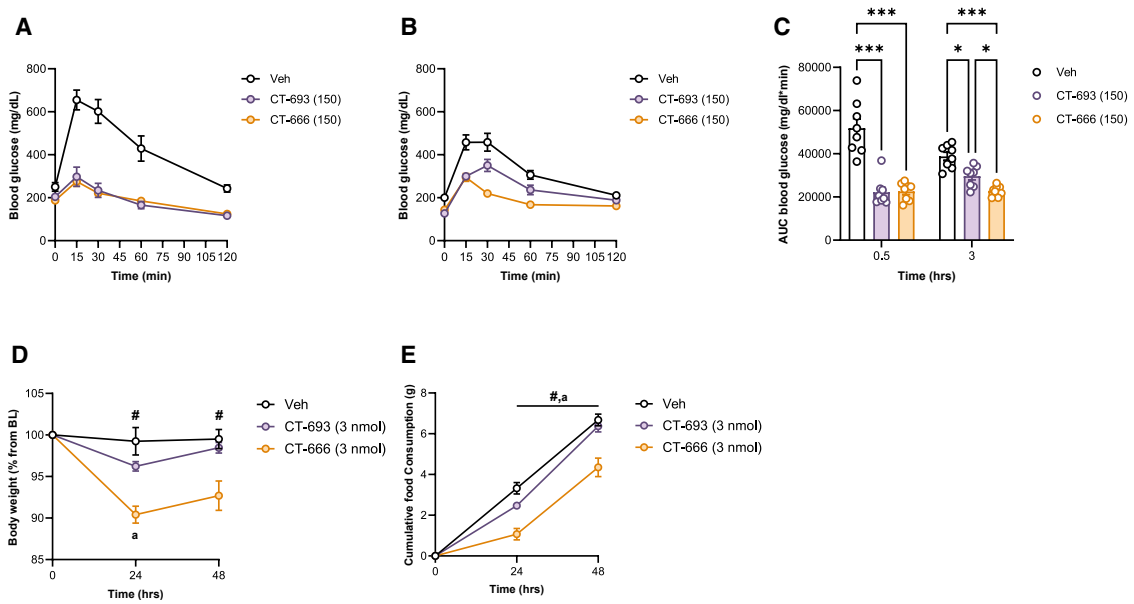

Figure 5. CT-666, a "biased" GIPR agonist, improved glucose tolerance over longer duration and decreased body weight more than CT-693, an "unbiased" GIPR agonist

(A–C) Mean (±SE) glucose response to an ipGTT (A) 30 min and (B) 3 h after vehicle (n = 8), CT-693 (150 nmol/kg; n = 8), and CT-666 (150 nmol/kg; n = 8) administration and the (C) corresponding area under the glucose curves.

(D and E) (D) Body weight and (E) food consumption after a single ICV injection of vehicle (n = 4), CT-693 (3 nmol; n = 6), and CT-666 (3 nmol; n = 6) in lean C57BL/6N mice.

Statistical differences were evaluated using a two-way ANOVA followed by Bonferroni post hoc test. *$p < 0.05$; ***$p < 0.001$; for (D and E), #$p < 0.05$: vehicle vs. CT-44666 (3 nmol), a = $p < 0.05$; CT-44693 (3 nmol) vs. CT-44666 (3 nmol).

at 24 h, respectively). Interestingly, despite some degree of recovery for each individual agent, combining CT-859 and CT-666 resulted in further weight loss at 48 h (−16% vs. vehicle) that was sustained at 72 h (−11% vs. vehicle). This combined effect surpassed the sum of effects induced by each individual agent.

DISCUSSION

Since the introduction of the first GLP-1RA, the class of molecules has continually evolved to address adverse effect profile, duration of action, administration convenience, and efficacy. The advent of tirzepatide marked a significant leap in efficacy through acting on both GLP-1R and GIPR.[13,38] In addition, while it mimics the actions of native GIP at the GIP receptor, tirzepatide exhibits bias at the GLP-1 receptor, favoring cAMP generation over β-arrestin recruitment.[16] This biased signaling led to significantly less GLP-1R internalization (E_{max}: 43.6% of GLP-1).[16] CT-859 is also a dual GLP-1R/GIPR agonist but exhibits bias on both receptors in favor of cAMP generation over β-arrestin recruitment. In fact, the bias is more complete (<5% β-arrestin recruitment), and interestingly, CT-859 not only avoids inducing receptor internalization but also may act as an antagonist of β-arrestin coupling, maintaining receptors to the cell membrane.

These *in vitro* characteristics seem to translate into improved *in vivo* efficacy, as demonstrated by CT-859 potently lowering glucose during an ipGTT with an ED_{50} of 0.46 nmol/kg, despite being less potent than native ligand GLP-1 and liraglutide on GLP-1R. When comparing CT-859 to liraglutide, CT-859 showed much-prolonged glucose reduction in both lean and DIO mice. While the mouse models used in this study were euglycemic, we consistently observed a reduction in glucose excursion upon CT-859 treatment. We anticipate similar benefits in a dysglycemic model, which will be assessed in future studies. The prolonged efficacy was not due to additional engagement of GIPR, as CT-859 was administered at a non-GIPR-engaging dose, and the observation was consistent in GIPR knockout mice. Nor can it be explained by circulating drug concentrations, as liraglutide at equal molar doses exhibits much greater (6-fold) drug exposure. These results imply that the improved efficacy is likely mediated through the biased signaling activation of GLP-1R. Supporting this, a number of studies have demonstrated that biased GLP-1R agonists are more efficacious than unbiased GLP-1R agonists on glucose regulation.[19–22] This is further corroborated by recent studies in adult β cell-specific β-arrestin 2 knockout mice showing that prolonged exposure to GLP-1R agonists, for 6 h or longer, increases glucose-lowering capacity by increasing insulin secretion.[27] Taken together, these results support that the absence of β-arrestin coupling enhances the efficacy of GLP-1 receptor agonists on glucose control.

These acute setting observations seemed to translate into enhanced efficacy in a sub-chronic setting, which holds more relevance in the field of diabetes and obesity. In a 3-week study comparing CT-859 to liraglutide at a non-GIPR-engaging dose in DIO mice, significantly greater BG reduction and improvement of HOMA-IR were obtained with CT-859 treatments. More

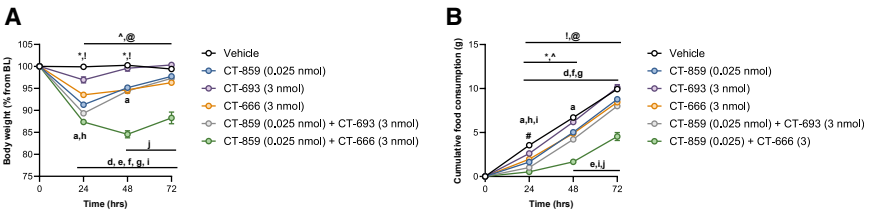

Figure 6. Central administration of CT-666 enhances the body weight reduction of a non-GIPR-engaging dose of CT-859

Mean (±SE) (A) body weight and (B) food consumption after a single ICV injection of vehicle ($n = 7$), CT-859 (0.025 nmol; $n = 8$), CT-693 (3 nmol; $n = 7$), CT-666 (3 nmol; $n = 8$), CT-859 (0.025 nmol) + CT-693 (3 nmol; $n = 7$), and CT-859 (0.025 nmol) + CT-666 (3 nmol; $n = 7$).

Statistical differences were evaluated using a two-way ANOVA followed by Bonferroni post hoc test. *$p < 0.05$; vehicle vs. CT-859 (0.025 nmol), #$p < 0.05$; vehicle vs. CT-693 (3 nmol), ^$p < 0.05$; vehicle vs. CT-666 (3 nmol), ! = $p < 0.05$; vehicle vs. CT-859 (0.025 nmol) + CT-693 (3 nmol), @ = $p < 0.05$; vehicle vs. CT-859 (0.025 nmol) + CT-666 (3 nmol), a = $p < 0.05$; CT-859 (0.025 nmol) vs. CT-693 (3 nmol), d = 0.05; CT-859 (0.025 nmol) vs. CT-859 (0.025 nmol) + CT-666 (3 nmol), e = $p < 0.05$; CT-693 (3 nmol) vs. CT-666 (3 nmol), f = $p < 0.05$; CT-693 (3 nmol) vs. CT-859 (0.025 nmol) + CT-693 (3 nmol), g = $p < 0.05$; CT-693 (3 nmol) vs. CT-859 (0.025 nmol) + CT-666 (3 nmol), h = $p < 0.05$; CT-666 (3 nmol) vs. CT-859 (0.025 nmol) + CT-693 (3 nmol), i = $p < 0.05$; CT-666 (3 nmol) vs. CT-859 (0.025 nmol) + CT-666 (3 nmol), j = $p < 0.05$; CT-859 (0.025 nmol) + CT-693 (3 nmol) vs. CT-859 (0.025 nmol) + CT-44666 (3 nmol).

importantly, CT-859 led to more substantial weight loss, with the difference between treatments becoming increasingly pronounced as the study progressed. Interestingly, in this sub-chronic setting, CT-859 and liraglutide achieved comparable suppression of food intake. This observation suggests that while appetite suppression may contribute to weight loss for both molecules, there may be additional mechanisms involved. For instance, GLP-1R agonists have been shown to stimulate brown adipose tissue thermogenesis and promote adipocyte browning independent of nutrient intake in mice.[39,40] Additionally, in a longitudinal study involving patients with obesity and T2D, 1-year liraglutide treatment increased energy expenditure.[41] Whether biased signaling with CT-859 on GLP-1R can maintain or even enhance this thermogenic mechanism remains to be investigated.

The impact of biased GLP-1R agonism on glucose regulation efficacy has been consistently observed, yet its effects on appetite and body weight regulation have shown variability across different biased GLP-1R agonists.[17–22] Most evaluations of biased GLP-1R agonists have utilized peripheral administration, raising the question of whether differences in brain bioavailability could explain the inconsistent responses observed. GLP-1R agonists are typically derivatized by half-life-extending lipid modifications on lysine residues to extend their durability. These lipid modifications can alter the bioavailability of the GLP-1R agonists in the brain, as the nature of the modification impacts the ability of these agonists to cross the blood-brain barrier (BBB). Short-acting GLP-1R agonists such as Ex-4 are mainly detectable outside the BBB; however, GLP-1R agonists with half-life-extending modifications are detected in areas of the brain beyond the BBB, with the spread being associated with the chain length of the lipid modification.[42] The ability of GLP-1R agonists to cross the BBB is essential because studies that inhibited or knocked down/out neuronal GLP-1R demonstrated that the anorectic and weight loss effects of GLP-1R agonists are mediated mainly by the central nervous system (CNS).[32,33,43] Many factors can alter the bioavailability of GLP-1R agonists in the brain, such as GLP-1R expression, glycemia, and obesity.[44,45] Therefore, to eliminate variations in how different compounds are absorbed in the brain, we administered compounds through an ICV injection. This approach allowed us to directly assess the differences in food intake and body weight reduction between biased and unbiased GLP-1R agonists. Indeed, we were able to differentiate the efficacy of CT-859 at doses that do not engage GIPR from liraglutide with ICV administration. As a further confirmation, ICV administration of Ex-Phe1, a known cAMP-biased GLP-1R agonist, resulted in greater appetite suppression and weight loss when compared to Ex-4. Notably, these effects were not observed with peripheral administration,[19,21,22] suggesting that the degree of access to central GLP-1Rs is crucial. Our data clearly demonstrated that, compared to an unbiased GLP-1R agonist (liraglutide), biased activation of GLP-1R can lead to superior regulation of glucose and body weight, provided that the agonists can reach the receptors in the respective target tissues. We also understand that the neuronal populations activated may not be the same between peripheral administration and an ICV injection. Future studies should examine neuronal activation between biased and unbiased agonists to ensure that ICV administration leads to activation of the same neurons.

CT-859 is a dual agonist for both GLP-1R and GIPR, with GIPR engagement occurring at higher doses. To assess the full efficacy capacity of CT-859, we evaluated sub-chronic dosing in DIO mice against liraglutide at 200 nmol/kg, which is a dose that activates both GLP-1R and GIPR for CT-859 and is a relatively high dose for liraglutide. Treatment with both molecules led to significant weight loss; however, the reduction with CT-859 was much more pronounced, a ~33% decrease compared to vehicle, whereas liraglutide achieved a ~22% reduction. This additional 10% weight loss with CT-859 likely stems from its biased GLP-1R agonism combined with the activation of GIPR. Interestingly, CT-859 also led to significantly greater suppression of food intake on day 7 compared to liraglutide at this dosage. Additionally, in a separate study, CT-859 at this dose decreased body weight more than a 60% caloric-restricted group even though cumulative food intake was not different between the groups. This raises the question: is GIPR engagement contributing to this outcome? The role of GIPR in energy and weight regulation remains a topic of debate.[36,37]

To address the question of whether biased signaling toward cAMP generation over β-arrestin recruitment at the GIPR alters *in vivo* efficacy, we opted for central administration of GIPR agonists to dissect the role of GIPR directly, positing that GIPR in the CNS is the key mediator for food intake suppression. To this end, two GIPR agonists were engineered, CT-693, which induces balanced cAMP and β-arrestin signaling, and CT-666, a cAMP-biased agonist that does not promote β-arrestin recruitment. Consistent with biased GLP-1R agonists, CT-666 does not

induce receptor internalization and, more importantly, outperforms CT-693 in appetite suppression and body weight reduction when administered centrally. Building on this, we combined these GIPR agonists with CT-859 at a non-GIPR-engaging dose in a subsequent study. Again, the biased GIPR agonist CT-666 was superior to unbiased CT-693 in enhancing the efficacy of CT-859. This confirms that central activation of GIPR plays a significant role in regulating energy consumption and weight loss, with biased GIPR agonists achieving markedly better efficacy. These results indicate that biased signaling should be considered when designing incretin therapeutics for treating obesity, as biased agonists may be more efficacious at suppressing food intake and lowering body weight. There has been great interest in the role of β-arrestin in GIPR signaling and efficacy. Several studies have reported that genetic ablation of β-arrestin in either isolated pancreatic β cells or mice resulted in a loss of GIP-induced insulin secretion and glucose regulation.[16,24,25] This highlights a genetic requirement for β-arrestin expression for GIPR *in vivo* function. However, it cannot be ruled out that GIPR function is indirectly affected as a developmental consequence of β-arrestin knockout. Indeed, β-arrestin-1 promotes β cell proliferation and protection from apoptosis.[46,47] In contrast to the hypothesis that β-arrestin signaling is required to obtain GIPR functional signaling, pharmacological agents that are cAMP-biased GIPR agonists exhibit significantly greater glucose-stimulated insulin secretion in a rat insulinoma cell line.[26] Our findings further illustrate that pharmacological manipulations provide different insights than can be obtained with genetic manipulations. Of course, both methods have their limitations, and future studies are planned to tease out these issues.

Conclusion

In this study, we observed that biased agonism of the GLP-1R results in improved glycemic control. Additionally, our findings further define the role of biased GLP-1R cAMP signaling in food consumption and body weight regulation. Biased GLP-1R agonism leads to greater suppression of food intake and promotion of weight loss. Furthermore, our data establish a role of biased cAMP signaling through the GIPR in glycemic homeostasis, food consumption, and weight loss. Like GLP-1R, biased GIPR agonism enhances efficacy. Finally, our data show that concerted biased engagement of both GLP-1R and GIPR leads to greater efficacy. Biased, dual activation of GLP-1R and GIPR, whether through a combination of individual agonists or a dual-function molecule like CT-859, offers promising therapeutic potential in the treatment of T2D and obesity.

Limitations of the study

There is the possibility that the use of tagged receptors and effectors in recombinant cells could result in artificial results when conducting *in vitro* assays. To rule out the impact of the tags on receptor function, we assessed native ligand-stimulated cAMP accumulation of the tagged receptors used in these studies and report those results in our method details. Future studies will address this caveat by minimizing the modifications of the receptor, utilizing endogenously expressing receptors in nonrecombinant cell lines, and interrogating alternate mechanisms of action.

The difference in weight loss between CT-859 and liraglutide at 20 and 200 nmol/kg may result from other mechanisms other than suppression of food intake. Therefore, future studies will examine the contribution of energy expenditure, activity, and other potential mechanisms to the observed effects of CT-859. Although CT-859 is a biased dual GLP-1R/GIPR agonist, it is much more potent on the GLP-1R with an ipGTT ED_{50} of 0.46 nmol/kg, whereas full GIPR engagement is seen at 200 nmol/kg. The difference in receptor engagement makes it very challenging to tease out the contribution of the GIPR to the observed effects on food intake and weight loss. Future studies will use a more balanced dual GLP-1R/GIPR agonist and use both GLP-1R$^{-/-}$ and GIPR$^{-/-}$ to tease out how each receptor contributes to the synergistic effects of a dual GLP-1R/GIPR agonist.

Evaluating food intake after ICV administration may not be physiologically relevant, as this route of administration does not accurately mimic the normal physiological pathway of compounds that are administered peripherally. Future studies would incorporate both methods to better distinguish between central and peripheral effects, providing a more complete understanding of how our compounds influence food intake and metabolic regulation.

RESOURCE AVAILABILITY

Lead contact

Further information and requests for resources and reagents should be directed to and will be fulfilled by the lead contact, Manu V. Chakravarthy (chakram5@gene.com).

Materials availability

All unique/stable reagents generated in this study are available from the lead contact with a completed materials transfer agreement.

Data and code availability

- All data reported in this paper will be shared by the lead contact upon request.
- This paper does not report original code.
- Any additional information required to reanalyze the data reported in this paper is available from the lead contact upon request.

ACKNOWLEDGMENTS

We would like to thank Andrew M. Sawayama, David J. Lloyd, and Jeff S. Iwig for their contributions to the discovery, development, and characterization of CT-859.

AUTHOR CONTRIBUTIONS

Conceptualization, R.R., A.H., J.L., S.K.H., and M.V.C.; methodology, R.R., A. H., D. Bone, R.F., J.L., S.K.H., M.V.C., S.K., D.A.E., T. Tang., and C.L.; investigation, R.R., A.H., M.M., D.L., T. Tracy., J.E., A. Pant, and A. Patton; writing – original draft, R.R., A.H., S.K., D. Bone, and J.L.; writing – review and editing, R. R., A.H., S.K.H., M.M., D.L., T. Tracy., T. Tang., A. Pant, C.L., A. Patton, J.E., D. Bone, R.F., D. Bialonczyk, J.L., S.K.H., and M.V.C.; funding acquisition, S.K.H. and M.V.C.; resources, T. Tang. and C.L.; supervision, R.R., A.H., S.K., D. Bone, D. Bialonczyk, J.L., S.K.H., and M.V.C.

DECLARATION OF INTERESTS

All authors are current or past employees of Carmot Therapeutics.

STAR★METHODS

Detailed methods are provided in the online version of this paper and include the following:

- KEY RESOURCES TABLE
- EXPERIMENTAL MODEL AND STUDY PARTICIPANT DETAILS
  - Mice
- METHOD DETAILS
  - Peptide synthesis general procedures
  - Cleavage and work-up procedures
  - Purification conditions
  - Preparative HPLC condition P1
  - Preparative HPLC condition P2
  - Preparative HPLC condition P3
  - Preparative HPLC condition P4
  - Analytical HPLC conditions A1
  - Analytical HPLC conditions A2
  - LC-MS conditions L1
  - Preparation of CT-859
  - Preparation of CT-666
  - Preparation of CT-693
  - Preparation of Ex-Phe1
  - cAMP Production
  - β-arrestin 2 recruitment
  - Internalization
  - Intraperitoneal glucose tolerance test
  - Food consumption
  - Intracerebroventricular cannulations
  - Weight loss
  - Caloric restriction
  - Pharmacokinetics
  - Plasma insulin
- QUANTIFICATION AND STATISTICAL ANALYSIS

SUPPLEMENTAL INFORMATION

Supplemental information can be found online at https://doi.org/10.1016/j.xcrm.2025.102156.

Received: June 19, 2024
Revised: November 15, 2024
Accepted: May 6, 2025
Published: June 2, 2025

REFERENCES

1. Fryar, C.D., Carroll, M.D., and Afful, J.. Prevalence of overweight, obesity, and severe obesity among adults aged 20 and over: United States, 1960–1962 through 2017–2018. NCHS Health E-Stats. https://www.cdc.gov/nchs/data/hestat/obesity-adult-17-18/obesity-adult.htm.
2. QuickStats: Age-Adjusted Prevalence of Total, Diagnosed, and Undiagnosed Diabetes Among Adults Aged ≥20 Years — National Health and Nutrition Examination Survey, 1999–2000 to 2015–2016. (2018). https://www.cdc.gov/diabetes/php/data-research/index.html.
3. Pi-Sunyer, X., Astrup, A., Fujioka, K., Greenway, F., Halpern, A., Krempf, M., Lau D.C.W., le Roux C.W., Violante Ortiz, R., Jensen C.B., and Wilding J.P.H.. A Randomized, Controlled Trial of 3.0 mg of Liraglutide in Weight Management. 373, 11–22. https://doi.org/10.1056/NEJMoa1411892.
4. Ahmann, A.J., Capehorn, M., Charpentier, G., Dotta, F., Henkel, E., Lingvay, I., Holst, A.G., Annett, M.P., and Aroda, V.R. (2018). Efficacy and Safety of Once-Weekly Semaglutide Versus Exenatide ER in Subjects With Type 2 Diabetes (SUSTAIN 3): A 56-Week, Open-Label, Randomized Clinical Trial. Diabetes Care 41, 258–266. https://doi.org/10.2337/dc17-0417.
5. Wilding, J.P.H., Batterham, R.L., Calanna, S., Davies, M., Van Gaal, L.F., Lingvay, I., McGowan, B.M., Rosenstock, J., Tran, M.T.D., Wadden, T.A., et al. (2021). Once-Weekly Semaglutide in Adults with Overweight or Obesity. N. Engl. J. Med. *384*, 989–1002. https://doi.org/10.1056/NEJMoa2032183.
6. Russell-Jones, D., Vaag, A., Schmitz, O., Sethi, B.K., Lalic, N., Antic, S., Zdravkovic, M., Ravn, G.M., and Simó, R.; Liraglutide Effect and Action in Diabetes 5 LEAD-5 met+SU Study Group (2009). Liraglutide vs insulin glargine and placebo in combination with metformin and sulfonylurea therapy in type 2 diabetes mellitus (LEAD-5 met+SU): a randomised controlled trial. Diabetologia *52*, 2046–2055. https://doi.org/10.1007/s00125-009-1472-y.
7. Hjørne, A.P., Modvig, I.M., and Holst, J.J. (2022). The Sensory Mechanisms of Nutrient-Induced GLP-1 Secretion. Metabolites *12*, 420.
8. Kuhre, R.E., Frost, C.R., Svendsen, B., and Holst, J.J. (2015). Molecular Mechanisms of Glucose-Stimulated GLP-1 Secretion From Perfused Rat Small Intestine. Diabetes *64*, 370–382. https://doi.org/10.2337/db14-0807.
9. Sun, E.W., de Fontgalland, D., Rabbitt, P., Hollington, P., Sposato, L., Due, S.L., Wattchow, D.A., Rayner, C.K., Deane, A.M., Young, R.L., and Keating, D.J. (2017). Mechanisms Controlling Glucose-Induced GLP-1 Secretion in Human Small Intestine. Diabetes *66*, 2144–2149. https://doi.org/10.2337/db17-0058.
10. Iwasaki, K., Harada, N., Sasaki, K., Yamane, S., Iida, K., Suzuki, K., Hamasaki, A., Nasteska, D., Shibue, K., Joo, E., et al. (2015). Free Fatty Acid Receptor GPR120 Is Highly Expressed in Enteroendocrine K Cells of the Upper Small Intestine and Has a Critical Role in GIP Secretion After Fat Ingestion. Endocrinology *156*, 837–846. https://doi.org/10.1210/en.2014-1653.
11. Nauck, M.A., Homberger, E., Siegel, E.G., Allen, R.C., Eaton, R.P., Ebert, R., and Creutzfeldt, W. (1986). Incretin effects of increasing glucose loads in man calculated from venous insulin and C-peptide responses. J. Clin. Endocrinol. Metab. *63*, 492–498. https://doi.org/10.1210/jcem-63-2-492.
12. Samms, R.J., Coghlan, M.P., and Sloop, K.W. (2020). How May GIP Enhance the Therapeutic Efficacy of GLP-1? Trends Endocrinol. Metab. *31*, 410–421. https://doi.org/10.1016/j.tem.2020.02.006.
13. Coskun, T., Sloop, K.W., Loghin, C., Alsina-Fernandez, J., Urva, S., Bokvist, K.B., Cui, X., Briere, D.A., Cabrera, O., Roell, W.C., et al. (2018). LY3298176, a novel dual GIP and GLP-1 receptor agonist for the treatment of type 2 diabetes mellitus: From discovery to clinical proof of concept. Mol. Metab. *18*, 3–14. https://doi.org/10.1016/j.molmet.2018.09.009.
14. Frías, J.P., Davies, M.J., Rosenstock, J., Pérez Manghi, F.C., Fernández Landó, L., Bergman, B.K., Liu, B., Cui, X., and Brown, K. (2021). Tirzepatide versus Semaglutide Once Weekly in Patients with Type 2 Diabetes. N. Engl. J. Med. Overseas. Ed. *385*, 503–515. https://doi.org/10.1056/NEJMoa2107519.
15. Jastreboff, A.M., Aronne, L.J., Ahmad, N.N., Wharton, S., Connery, L., Alves, B., Kiyosue, A., Zhang, S., Liu, B., Bunck, M.C., et al. (2022). Tirzepatide Once Weekly for the Treatment of Obesity. N. Engl. J. Med. *387*, 205–216. https://doi.org/10.1056/NEJMoa2206038.
16. Willard, F.S., Douros, J.D., Gabe, M.B.N., Showalter, A.D., Wainscott, D.B., Suter, T.M., Capozzi, M.E., van der Velden, W.J.C., Stutsman, C., Cardona, G.R., et al. (2020). Tirzepatide is an imbalanced and biased dual GIP and GLP-1 receptor agonist. JCI Insight *5*, 10. https://doi.org/10.1172/jci.insight.140532.
17. Guo, W., Xu, Z., Zou, H., Li, F., Li, Y., Feng, J., Zhu, Z., Zheng, Q., Zhu, R., Wang, B., et al. (2023). Discovery of ecnoglutide - A novel, long-acting, cAMP-biased glucagon-like peptide-1 (GLP-1) analog. Mol. Metab. *75*, 101762. https://doi.org/10.1016/j.molmet.2023.101762.
18. Hinds, C.E., Peace, E., Chen, S., Davies, I., El Eid, L., Tomas, A., Tan, T., Minnion, J., Jones, B., and Bloom, S.R. (2024). Abolishing β-arrestin recruitment is necessary for the full metabolic benefits of G protein-biased glucagon-like peptide-1 receptor agonists. Diabetes Obes. Metab. *26*, 65–77. https://doi.org/10.1111/dom.15288.

19. Jones, B., Buenaventura, T., Kanda, N., Chabosseau, P., Owen, B.M., Scott, R., Goldin, R., Angkathunyakul, N., Corrêa, I.R., Jr., Bosco, D., et al. (2018). Targeting GLP-1 receptor trafficking to improve agonist efficacy. Nat. Commun. *9*, 1602. https://doi.org/10.1038/s41467-018-03941-2.

20. Lucey, M., Pickford, P., Bitsi, S., Minnion, J., Ungewiss, J., Schoeneberg, K., Rutter, G.A., Bloom, S.R., Tomas, A., and Jones, B. (2020). Disconnect between signalling potency and in vivo efficacy of pharmacokinetically optimised biased glucagon-like peptide-1 receptor agonists. Mol. Metab. *37*, 100991. https://doi.org/10.1016/j.molmet.2020.100991.

21. Pickford, P., Lucey, M., Fang, Z., Bitsi, S., de la Serna, J.B., Broichhagen, J., Hodson, D.J., Minnion, J., Rutter, G.A., Bloom, S.R., et al. (2020). Signalling, trafficking and glucoregulatory properties of glucagon-like peptide-1 receptor agonists exendin-4 and lixisenatide. Br. J. Pharmacol. *177*, 3905–3923. https://doi.org/10.1111/bph.15134.

22. Zhang, H., Sturchler, E., Zhu, J., Nieto, A., Cistrone, P.A., Xie, J., He, L., Yea, K., Jones, T., Turn, R., et al. (2015). Autocrine selection of a GLP-1R G-protein biased agonist with potent antidiabetic effects. Nat. Commun. *6*, 8918. https://doi.org/10.1038/ncomms9918.

23. El, K., Douros, J.D., Willard, F.S., Novikoff, A., Sargsyan, A., Perez-Tilve, D., Wainscott, D.B., Yang, B., Chen, A., Wothe, D., et al. (2023). The incretin co-agonist tirzepatide requires GIPR for hormone secretion from human islets. Nat. Metab. *5*, 945–954. https://doi.org/10.1038/s42255-023-00811-0.

24. Zaimia, N., Obeid, J., Varrault, A., Sabatier, J., Broca, C., Gilon, P., Costes, S., Bertrand, G., and Ravier, M.A. (2023). GLP-1 and GIP receptors signal through distinct beta-arrestin 2-dependent pathways to regulate pancreatic beta cell function. Cell Rep. *42*, 10. https://doi.org/10.1016/j.celrep.2023.113326.

25. Kizilkaya, H.S., Sørensen, K.V., Madsen, J.S., Lindquist, P., Douros, J.D., Bork-Jensen, J., Berghella, A., Gerlach, P.A., Gasbjerg, L.S., Mokrosiński, J., et al. (2024). Characterization of genetic variants of GIPR reveals a contribution of β-arrestin to metabolic phenotypes. Nat. Metab. *6*, 1268–1281. https://doi.org/10.1038/s42255-024-01061-4.

26. Jones, B., McGlone, E.R., Fang, Z., Pickford, P., Corrêa, I.R., Jr., Oishi, A., Jockers, R., Inoue, A., Kumar, S., Görlitz, F., et al. (2021). Genetic and biased agonist-mediated reductions in beta-arrestin recruitment prolong cAMP signaling at glucagon family receptors. J. Biol. Chem. *296*, 100133. https://doi.org/10.1074/jbc.RA120.016334.

27. Bitsi, S., El Eid, L., Manchanda, Y., Oqua, A.I., Mohamed, N., Hansen, B., Suba, K., Rutter, G.A., Salem, V., Jones, B., and Tomas, A. (2023). Divergent acute versus prolonged pharmacological GLP-1R responses in adult β cell-specific β-arrestin 2 knockout mice. Sci. Adv. *9*, eadf7737. https://doi.org/10.1126/sciadv.adf7737.

28. Harris, M., Mackie, D.I., Pawlak, J.B., Carvalho, S., Truong, T.T., Safitri, D., Yeung, H.Y., Routledge, S., Harper, M.T., Al-Zaid, B., et al. (2021). RAMPs regulate signalling bias and internalisation of the GIPR. Preprint at bioRxiv. https://doi.org/10.1101/2021.04.08.436756.

29. Gabe, M.B.N., Sparre-Ulrich, A.H., Pedersen, M.F., Gasbjerg, L.S., Inoue, A., Bräuner-Osborne, H., Hartmann, B., and Rosenkilde, M.M. (2018). Human GIP(3-30)NH(2) inhibits G protein-dependent as well as G protein-independent signaling and is selective for the GIP receptor with high-affinity binding to primate but not rodent GIP receptors. Biochem. Pharmacol. *150*, 97–107. https://doi.org/10.1016/j.bcp.2018.01.040.

30. Gasbjerg, L.S., Rasmussen, R.S., Dragan, A., Lindquist, P., Melchiorsen, J.U., Stepniewski, T.M., Schiellerup, S., Tordrup, E.K., Gadgaard, S., Kizilkaya, H.S., et al. (2024). Altered desensitization and internalization patterns of rodent versus human glucose-dependent insulinotropic polypeptide (GIP) receptors. An important drug discovery challenge. Br. J. Pharmacol., 1–18. https://doi.org/10.1111/bph.16478.

31. Yang, B., Gelfanov, V.M., El, K., Chen, A., Rohlfs, R., DuBois, B., Kruse Hansen, A.M., Perez-Tilve, D., Knerr, P.J., D'Alessio, D., et al. (2022). Discovery of a potent GIPR peptide antagonist that is effective in rodent and human systems. Mol. Metab. *66*, 101638. https://doi.org/10.1016/j.molmet.2022.101638.

32. Sisley, S., Gutierrez-Aguilar, R., Scott, M., D'Alessio, D.A., Sandoval, D.A., and Seeley, R.J. (2014). Neuronal GLP1R mediates liraglutide's anorectic but not glucose-lowering effect. J. Clin. Investig. *124*, 2456–2463. https://doi.org/10.1172/JCI72434.

33. Secher, A., Jelsing, J., Baquero, A.F., Hecksher-Sørensen, J., Cowley, M.A., Dalbøge, L.S., Hansen, G., Grove, K.L., Pyke, C., Raun, K., et al. (2014). The arcuate nucleus mediates GLP-1 receptor agonist liraglutide-dependent weight loss. J. Clin. Investig. *124*, 4473–4488. https://doi.org/10.1172/JCI75276.

34. Reiner, D.J., Mietlicki-Baase, E.G., McGrath, L.E., Zimmer, D.J., Bence, K.K., Sousa, G.L., Konanur, V.R., Krawczyk, J., Burk, D.H., Kanoski, S.E., et al. (2016). Astrocytes Regulate GLP-1 Receptor-Mediated Effects on Energy Balance. J. Neurosci. *36*, 3531–3540. https://doi.org/10.1523/JNEUROSCI.3579-15.2016.

35. Adams, J.M., Pei, H., Sandoval, D.A., Seeley, R.J., Chang, R.B., Liberles, S.D., and Olson, D.P. (2018). Liraglutide Modulates Appetite and Body Weight Through Glucagon-Like Peptide 1 Receptor-Expressing Glutamatergic Neurons. Diabetes *67*, 1538–1548. https://doi.org/10.2337/db17-1385.

36. Killion, E.A., Lu, S.-C., Fort, M., Yamada, Y., Véniant, M.M., and Lloyd, D.J. (2020). Glucose-Dependent Insulinotropic Polypeptide Receptor Therapies for the Treatment of Obesity, Do Agonists = Antagonists? Endocr. Rev. *41*, bnz002–21. https://doi.org/10.1210/endrev/bnz002.

37. Campbell, J.E. (2021). Targeting the GIPR for obesity: To agonize or antagonize? Potential mechanisms. Mol. Metab. *46*, 101139. https://doi.org/10.1016/j.molmet.2020.101139.

38. Samms, R.J., Christe, M.E., Collins, K.A., Pirro, V., Droz, B.A., Holland, A.K., Friedrich, J.L., Wojnicki, S., Konkol, D.L., Cosgrove, R., et al. (2021). GIPR agonism mediates weight-independent insulin sensitization by tirzepatide in obese mice. J. Clin. Investig. *131*, e146353. https://doi.org/10.1172/JCI146353.

39. Martins, F.F., Marinho, T.S., Cardoso, L.E.M., Barbosa-da-Silva, S., Souza-Mello, V., Aguila, M.B., and Mandarim-de-Lacerda, C.A. (2022). Semaglutide (GLP-1 receptor agonist) stimulates browning on subcutaneous fat adipocytes and mitigates inflammation and endoplasmic reticulum stress in visceral fat adipocytes of obese mice. Cell Biochem. Funct. *40*, 903–913. https://doi.org/10.1002/cbf.3751.

40. Gutierrez, A.D., Gao, Z., Hamidi, V., Zhu, L., Saint Andre, K.B., Riggs, K., Ruscheinsky, M., Wang, H., Yu, Y., Miller, C., 3rd., et al. (2022). Anti-diabetic effects of GLP1 analogs are mediated by thermogenic interleukin-6 signaling in adipocytes. Cell Rep. Med. *3*, 100813. https://doi.org/10.1016/j.xcrm.2022.100813.

41. Beiroa, D., Imbernon, M., Gallego, R., Senra, A., Herranz, D., Villarroya, F., Serrano, M., Fernø, J., Salvador, J., Escalada, J., et al. (2014). GLP-1 agonism stimulates brown adipose tissue thermogenesis and browning through hypothalamic AMPK. Diabetes *63*, 3346–3358. https://doi.org/10.2337/db14-0302.

42. Skovbjerg, G., Roostalu, U., Salinas, C.G., Skytte, J.L., Perens, J., Clemmensen, C., Elster, L., Frich, C.K., Hansen, H.H., and Hecksher-Sorensen, J. (2023). Uncovering CNS access of lipidated exendin-4 analogues by quantitative whole-brain 3D light sheet imaging. Neuropharmacology *238*, 10. https://doi.org/10.1016/j.neuropharm.2023.109637.

43. Fortin, S.M., Lipsky, R.K., Lhamo, R., Chen, J., Kim, E., Borner, T., Schmidt, H.D., and Hayes, M.R. (2020). GABA neurons in the nucleus tractus solitarius express GLP-1 receptors and mediate anorectic effects of liraglutide in rats. Sci. Transl. Med. *12*, eaay8071. https://doi.org/10.1126/scitranslmed.aay8071.

44. Imbernon, M., Saponaro, C., Helms, H.C.C., Duquenne, M., Fernandois, D., Deligia, E., Denis, R.G.P., Chao, D.H.M., Rasika, S., Staels, B., et al. (2022). Tanycytes control hypothalamic liraglutide uptake and its anti-obesity actions. Cell Metab. *34*, 1054–1063.e7. https://doi.org/10.1016/j.cmet.2022.06.002.

45. Bakker, W., Imbernon, M., Salinas, C.G., Moro Chao, D.H., Hassouna, R., Morel, C., Martin, C., Leger, C., Denis, R.G.P., Castel, J., et al. (2022). Acute changes in systemic glycemia gate access and action of GLP-1R agonist on brain structures controlling energy homeostasis. Cell Rep. *41*, 10. https://doi.org/10.1016/j.celrep.2022.111698.

46. Talbot, J., Joly, E., Prentki, M., and Buteau, J. (2012). beta-Arrestin1-mediated recruitment of c-Src underlies the proliferative action of glucagon-like peptide-1 in pancreatic beta INS832/13 cells. Mol. Cell. Endocrinol. *364*, 65–70. https://doi.org/10.1016/j.mce.2012.08.010.

47. Quoyer, J., Longuet, C., Broca, C., Linck, N., Costes, S., Varin, E., Bockaert, J., Bertrand, G., and Dalle, S. (2010). GLP-1 mediates antiapoptotic effect by phosphorylating Bad through a beta-arrestin 1-mediated ERK1/2 activation in pancreatic beta-cells. J. Biol. Chem. *285*, 1989–2002. https://doi.org/10.1074/jbc.M109.067207.

STAR★METHODS

KEY RESOURCES TABLE

REAGENT or RESOURCE	SOURCE	IDENTIFIER
Chemicals, peptides, and recombinant proteins		
IBMX	Sigma	45-I7018-1G-EA
Human GLP-1 (7–36)	Anaspec	AS-22463
Human GIP (1–42)	Anaspec	AS-61226-1
Liraglutide	SelleckChem	S8256
Exendin-4	Santa Cruz Biotech	Sc-474611
Potassium Phosphate Monobasic solution	Sigma-Aldrich	P8709-1L
Potassium phosphate dibasic solution	Sigma-Aldrich	P8584-1L
TWEEN® 20, PROTEIN GRADE	EMD Millipore Corp.	655206-50mL
Water, Optima LC/MS Grade	Fisher Scientific	W64
Saline	Pfizer	00409488810
Fmoc-β-alanine	Chem-Impex International	
Fmoc-*D*-alanine	Chem-Impex International	
4-(4-chlorophenyl)tetrahydro-2*H*-pyran-4-carboxylic acid	Enamine Ltd.	
Critical commercial assays		
HitHunter cAMP Assay for Biologics	Eurofins DiscoverX	90-0075LM
Nano-Glo® Live Cell Substrate	Promega	N2012
Nano-Glo® HiBiT Extracellular Detection System	Promega	N2421
Fugene 6	Promega	E2692
U-PLEX Mouse Insulin Assay	Meso Scale Discovery	K1526HK-2
Experimental models: Cell lines		
HEK293	ATCC	CRL-1573, (RRID:CVCL_0045)
CHO-K1	ATCC	CCL-61, (RRID:CVCL_0214)
CHO-K1 Snap-human GLP-1R Cell Line	Carmot	
CHO-K1 Snap-human GIPR Cell Line	Carmot	
CHO-K1 murine GIPR Gs Cell Line	Eurofins DiscoverX	(RRID:CVCL_KV50)
U2OS murine GLP-1R Gs Cell Line	Eurofins DiscoverX	(RRID:CVCL_KV95)
HEK293 human GLP-1R-LgBiT SmBiT-human-β-arrestin-2	Carmot	
HEK293 human GIPR-LgBiT SmBiT-human-β-arrestin-2	Carmot	
HEK293 mouse GLP-1R-LgBiT SmBiT-mouse-β-arrestin-2	Carmot	
HEK293 mouse GIPR-LgBiT SmBiT-mouse-β-arrestin-2	Carmot	
Experimental models: Organisms/strains		
C57BL/6J	The Jackson Laboratory	RRID:IMSR_JAX:000664
C57BL/6J DIO	The Jackson Laboratory	380050
C57BL/6-Glp1r^{em1_1Cgen}	Taconic Biosciences	
C57BL/6- Gt(ROSA)26Sor$^{tm16(cre)Arte}$ Gipr$^{em1.2Cgen}$	Taconic Biosciences	
Recombinant DNA		
SNAP-human GLP-1R	Cisbio	
SNAP-human GIPR	Cisbio	

(*Continued on next page*)

Continued

REAGENT or RESOURCE	SOURCE	IDENTIFIER
Homo sapiens GLP-1R-LgBiT	Promega	
Homo sapiens GIPR-LgBiT	Promega	
SmBiT- (Homo sapiens)-β-arrestin-2	Promega	
Mus musculus GLP-1R-LgBiT	Promega	
Mus musculus GIPR-LgBiT	Promega	
smBiT_(Mus musculus)- β-arrestin-2	Promega	
smBiT_(Mus musculus)- β-arrestin-1	Promega	
pcDNA3.1 (empty)	Genscript	
HiBiT-(human)-GLP-1R	Promega	
HiBiT-(human)-GIPR	Promega	
HiBiT-(Mus musculus)-GLP-1R	Promega/Genscript	
HiBiT-(Mus musculus)-GIPR	Promega/Genscript	
HiBiT-(Mus musculus)-GCGR	Promega/Genscript	
Software and algorithms		
Prism	GraphPad	
Excel	Microsoft	
Other		
Guide cannula	Protech International Inc.	C315GAS-5/SPC
Dummy cannula	Protech International Inc.	C315DCS-5/SPC
Internal cannula	Protech International Inc.	C315IAS-5/SPC
Stainless-steel screw	Protech International Inc.	
Dental cement	Stoelting	51458
Syringes	Hamilton Company, US	203073
Glucose meter	Data Sciences International	51073
Glucose strips	Data Sciences International	42214–100
Alpha Trak 3 Starter Kit	Zoetis	MWI 119405
AlphaTRAK 3 Test Strips	Zoetis	MWI 119409
Chow diet	Envigo-Teklad Diets	2920x
60% HFD	Research Diets, Inc	D12492 Q#1
50% dextrose	Vet one	NDC 13985-067-00

EXPERIMENTAL MODEL AND STUDY PARTICIPANT DETAILS

Mice

C57BL/6J and diet-induced obese (DIO) C57BL/6J male mice were obtained from The Jackson Laboratory. GLP-1R$^{+/+}$, GLP-1R$^{-/-}$, GIPR$^{+/+}$, and GIPR$^{-/-}$ male mice were obtained from Taconic Biosciences. Mice were singly housed under standard environmental conditions (22°C, 12h:12h light: dark cycle), with *ad libitum* access to water and regular chow (C57BL/6J; Teklad rodent diet 2920x, Inotiv) or HFD (DIO C57BL/6J; 60% kcal from fat, Research Diets #D12492) unless otherwise specified. Lean mice were used between 8 and 10 weeks of age. DIO mice were maintained on HFD for at least 18 weeks before experimentation. All studies were approved by FibroGen and Explora BioLabs' Institutional Animal Care and Use Committee.

METHOD DETAILS

Peptide synthesis general procedures

Unless otherwise specified, peptides were synthesized by microwave-assisted solid-phase peptide synthesis (SPPS) techniques using an Fmoc protection strategy on a Liberty Blue Microwave Peptide Synthesizer (CEM Corporation). Fmoc deprotections were carried out using 20% piperidine in 0.1 M Oxyma/DMF solution. Amino acid couplings were performed using a 5-fold excess of reagent; Fmoc-amino acids (0.2 M solution in DMF), DIC (0.5 or 1.0 M solution in DMF) and Oxyma (0.5 or 1.0 M solution in DMF) were employed on 0.05 or 0.1 mmol scale on Rink Amide ProTide Resin (LL).

Cleavage and work-up procedures

Unless otherwise specified, side chain protecting group removal with concomitant cleavage of peptide from the resin was carried out in a TFA/TIS/H_2O/PhOH (88:2:5:5 v/v/v/v) solution (10 mL/0.05 mmol) for 3 h at ambient temperature. Cold diethyl ether (30 mL/0.05 mmol) was used to precipitate the peptide, which was isolated by centrifugation (3000 rpm, 10 min).

Purification conditions

Crude peptide was iteratively purified by RP-HPLC until >95% purity was obtained. Purification conditions are listed as follows; suitable fractions were pooled and lyophilized. Peptide purity was determined by analytical RP-HPLC, and identity confirmed using LCMS.

Preparative HPLC condition P1

Column: Phenomenex Jupiter Proteo 90 Å 4 μm, 250 x 21.2 mm.
Solvent A = H2O with 0.1% TFA.
Solvent B = MeCN with 0.1% TFA.
Flow rate = 15 mL/min.
Column temperature: 20°C–25°C.
Gradient: 0–100% B over 30 min.

Time (min)	%A	%B
0	100	0
3	100	0
33	0	100
33.1	0	100
43	0	100
43.1	100	0
48	100	0

Preparative HPLC condition P2

Column: Phenomenex Aeris 5 μm Peptide XB-C18 250 × 21.2 mm AXIA packed.
Solvent A = H_2O with 20 mM NH4HCO3.
Solvent B = MeCN.
Flow rate = 15 mL/min.
Column temperature: 20°C–25°C.
Gradient: 20–50% B over 45 min.

Time (min)	%A	%B
0	100	0
0.1	95	5
2	80	20
47	50	50
47.1	0	100
57	0	100
57.1	100	0
61	100	0

Preparative HPLC condition P3

Column: Phenomenex Aeris 5 μm Peptide XB-C18 250 × 21.2 mm AXIA packed.
Solvent A = H_2O with 0.1% TFA.
Solvent B = MeCN with 0.1% TFA.
Flow rate = 25 mL/min.
Column temperature: 21°C.

Gradient: 20–40% B over 25 min.

Time (min)	%A	%B
0	100	0
0.25	95	5
2.50	80	20
27.50	60	40
27.51	0	100
32.50	0	100
32.51	100	0
35.00	100	0

Preparative HPLC condition P4

Column: Phenomenex Aeris 5 μm Peptide XB-C18 250 × 21.2 mm AXIA packed.
Solvent A = H_2O with 20 mM NH4HCO3.
Solvent B = MeCN.
Flow rate = 25 mL/min.
Column temperature: 21°C.
Gradient: 20–40% B over 25 min.

Time (min)	%A	%B
0	100	0
0.25	95	5
2.50	80	20
27.50	60	40
27.51	0	100
32.50	0	100
32.51	100	0
35.00	100	0

The purity of peptides was assessed by analytical RP-HPLC, and identity confirmed using LCMS with the following conditions.

Analytical HPLC conditions A1

Column: Waters XSelect CSHTM Prep C18 5 μm 3.0 x 150 mm.
Solvent A = H_2O with 0.1% TFA.
Solvent B = MeCN with 0.1% TFA.
Flow rate = 1 mL/min.
Column temperature: 21°C.
Wavelength: 214 nm.

Time (min)	%A	%B
0	95	5
3.00	70	30
23.00	45	55
24.00	5	95
33.00	5	95
33.10	95	5
35.00	95	5

Analytical HPLC conditions A2

Column: Waters XSelect CSHTM Prep C18 5 μm 3.0 x 150 mm.
Solvent A = H_2O with 0.1% TFA.
Solvent B = MeCN with 0.1% TFA.
Flow rate = 1 mL/min.
Column temperature: 21°C.
Wavelength: 214 nm.

Time (min)	%A	%B
0	95	5
3.00	70	30
23.00	50	50
24.00	5	95
33.00	5	95
33.10	95	5
35.00	95	5

LC-MS conditions L1

Column: Phenomenex Gemini 3 μm C19 110 Å LC Column 30 x 2 mm.
Solvent A = H_2O with 0.1% Formic Acid.
Solvent B = MeCN with 0.1% Formic Acid.
Flow rate = 0.9 mL/min.
Column temperature: 21°C.
Mass Range: 900–1500 m/z.

Time (min)	%A	%B
0.10	95	5
0.11	75	25
1.50	0	100
1.80	0	100
1.81	95	5
2.00	95	5

Preparation of CT-859

The reaction schemes for the preparation of CT-859 are depicted in Figure S8. To a slurry of hydrochloride salt *1* (9.83 g, 50 mmol) and thiodiglycolic anhydride *2* (6.61 g, 50 mmol, 1.0 equiv) in DMF (150 mL) was added DIPEA (34.8 mL, 4.0 equiv) at 23°C. The reaction mixture was stirred at ambient temperature for 30 min, at which point the reaction was deemed complete by RP-HPLC analysis. Compound *3* was carried forward for further transformations without purification.

CT-859 was prepared by Bachem Americas Inc. Resin-bound peptide intermediate *R-1* was prepared from Rink amide resin using Fmoc SPPS chemistry with α-Fmoc and sidechain protected canonical amino acid building blocks. Fmoc-(α-aminoisobutyric acid) and N^2-(((9*H*-fluoren-9-yl)methoxy)carbonyl)-N^6-((*S*)-5-(*tert*-butoxy)-5-oxo-4-palmitamidopentanoyl)-*L*-lysine were also employed in addition to standard amino acid building blocks.

To the separate solution of building block *3* in DMF, PyBOP (26.0 g, 1.0 equiv.) was added followed by DIPEA (17.4 mL, 2.0 equiv.). After stirring for 5 min at ambient temperature, the reaction mixture was added to resin *R-1* (14 mmol). The slurry was agitated for 4 h at ambient temperature and filtered. The resin was washed with DMF (3x), IPA (3x) and isopropyl ether (2x) and dried *in vacuo* to afford 128.6 g of product resin.

Side chain protecting group removal with concomitant cleavage from the resin was carried out in TFA/TIS/DODT/H_2O (90/5/2.5/2.5 v/v/v/v) for 3 h. The reaction slurry was filtered, the resin was washed with TFA, and the filtrate and washes were combined and diluted with pre-cooled isopropyl ether. The precipitated solids were collected by filtration and dried *in vacuo* to afford 44 g of the crude peptide.

The crude peptide was purified using a 2″ C18 column with a gradient of 0.05 M AcOH in H_2O/MeCN (flow rate = 100 mL/min), followed by salt exchange to the hydrochloride salt with 0.01 N HCl buffer (flow rate = 100 mL/min) on a 2″ C18 column. CT-859 hydrochloride (6 g) was afforded as a white powder (97% purity by Analytical HPLC), ESI-MS found 1543.9. $C_{212}H_{320}N_{47}O_{65}S_2$ $[M+3H]^{3+}$ requires 1543.9.

Preparation of CT-666

The structure of CT-666 is depicted in Figure S9A. CT-666 was synthesized, cleaved from resin, and worked-up at a 1.0 mmol scale following the general procedures with Fmoc-β-alanine and 4-(4-chlorophenyl)tetrahydro-2*H*-pyran-4-carboxylic acid as additional non-canonical building blocks. The crude peptide was dissolved in 2 mL of DMSO and iteratively purified following Preparative HPLC purification condition P3 until purity by analytical HPLC was >90%. Fractions of acceptable purity were lyophilized and resuspended in DMSO. The pH of the DMSO solution was modified by adding 1 mL of 200 nM NH_4HCO_3 in H_2O. Purification with Preparative HPLC condition P4 was followed and fractions with >95% purity were combined and lyophilized to afford CT-666 (109 mg) as a fluffy white solid, (>99% purity by Analytical HPLC Condition A2). ESI-MS found 1475.7; $C_{201}H_{299}ClN_{49}O_{60}S$ $[M+3H]^{3+}$ requires 1475.4.

Preparation of CT-693

The structure of CT-693 is depicted in Figure S9B. CT-693 was synthesized, cleaved from resin and worked-up at a 1.0 mmol scale following the general procedures with Fmoc-*D*-alanine as an additional non-canonical building block. Crude peptide was dissolved in 2 mL of DMSO and iteratively purified following preparative HPLC purification condition P3 until purity by analytical HPLC was >90%. Fractions were lyophilized and resuspended in DMSO. The pH of the DMSO solution was modified by adding 1 mL of 200 nM NH_4HCO_3 in H_2O. Purification with Preparative HPLC condition P4 was followed and fractions with >95% purity were combined and lyophilized to afford CT-693 (137 mg) as a white solid, (>99% purity by Analytical HPLC Condition A2). ESI-MS found 1455.9, $C_{198}H_{297}N_{50}O_{60}S$ $(M+3H)^{3+}$ requires 1455.7.

Preparation of Ex-Phe1

The structure of Ex-Phe1 is depicted in Figure S9C. Exendin-Phe1 (Ex-Phe1) was synthesized, cleaved from resin and worked-up at a 0.05 mmol scale following the general procedures with Fmoc-*D*-alanine as an additional non-canonical building block. The crude peptide was dissolved in DMSO/AcOH (1:1 v/v) and iteratively purified following Preparative HPLC purification condition P1 until purity by analytical HPLC was >90%. Fractions containing the peptide were lyophilized and resuspended in DMSO. Purification with Prep HPLC condition P2 was followed and fractions with >95% purity were combined and lyophilized to afford Ex-Phe1 (27.7 mg) as a white solid, (96% purity by Analytical HPLC Condition A2). ESI-MS found 1050.0, $C_{187}H_{288}N_{48}O_{60}S$ $[M+4H]^{4+}$ requires 1050.2.

cAMP Production

All cells were maintained in cell-specific media in a 37°C incubator at 5% CO_2. Cell lines were not authenticated but were confirmed mycoplasma free. Unless otherwise indicated, cAMP generation was measured using the HitHunter cAMP Assay kit. For mouse GLP-1R and GIPR, 10,000 cells per well were plated 24 h prior in assay complete cell plating reagent 2 (GIPR) or 5 (GLP-1R) in 384 well low-volume tissue culture treated plates. Before starting the assay, media was replaced with 5 μL assay buffer (1:2 ratio of anti-cAMP antibody: 1 x HBSS/10 mM HEPES/625 μM IBMX). For Snap-tagged human GLP-1R and GIPR and all other cAMP assays, cells were prepared in non-tissue culture treated plates the day of experiment in assay buffer. Where indicated, pGlosensor-22F (Promega) cAMP assays were conducted on either antibiotic selected stably expressing cells or 48 h Fugene 6 transiently transfected HEK293 cells and incubated in 10 μL 2% Glosensor (Promega) and CO2 independent media before compound addition. Compound dilutions were made 1:1 in DMSO, and then 5–10 nL was transferred to wells using an ECHO acoustic liquid handler (Labcyte). All assays were serum free. Plated cells were incubated for 30 min at room temperature. cAMP detection reagents were added according to the manufacturer's specifications, and luminescence was measured after the indicated incubation times using an EnVision Multimode Plate Reader (PerkinElmer). Data was normalized to 100% using wells receiving vehicle or high controls and Prism was used to generate nonlinear regression curve fits and figures.

To assess the effect of the tag on receptor signaling, HiBiT-tagged and LgBiT-tagged receptors were transiently transfected into pGlosensor-22F stably expressing HEK293 cell lines and cAMP accumulation in response to native ligand was measured 48 h after transfection. The EC50 (%Emax) of native ligand induced cAMP accumulation of HiBiT-tagged mouse and human GIPR was 0.005 pM (106%) and 0.002 pM (100%); HiBiT-tagged mouse and human GLP-1R was 0.005 pM (109%) and 0.002 pM (106%); LgBiT-tagged mouse and human GIPR was 0.111 pM (95%) and 0.086 pM (112%); and LgBiT-tagged mouse and human GLP-1R was 0.016 pM (103%), 0.021 pM (108%) respectively.

β-arrestin 2 recruitment

To measure GLP-1R and GIPR-mediated β-arrestin recruitment, we utilized Promega's NanoBiT technology or NanoLuc Binary Technology. The NanoLuc luciferase is split into two subunits, called LgBiT and SmBiT, which are expressed in HEK293 cells as fusion proteins at the C-terminus of GLP-1R or GIPR and the N-terminus of β-arrestin-1 or -2. Twenty-four hours before β-arrestin NanoBiT assays, cells were lifted with Cell Dissociation media and plated at 10,000 cells per well in TC-treated 384 low-volume plates. The next day, the media was removed and replaced with 10 μL 1:100 dilution of Nano-Glo Live Cell Substrate in Optimem

and equilibrated to room temperature for 10 min. Background luminescence was measured before 10 nL compound was added using an ECHO Acoustic Liquid Handler. Luminescence was measured at 1.5-min intervals for 30 min using an EnVision Multimode Plate Reader (PerkinElmer). All assays were set up such that each row of a 384 well plate contained a single dilution series and, for normalization purposes, a single low control well (vehicle-treated) and a single high control well (GLP-1 or GIP-treated).

Internalization

GLP-1R and GIPR internalization were measured using Promega's Nano-Glo HiBit extracellular detection system (Promega Corporation; Madison, WI). HEK293 cells were transiently transfected with HiBiT-tagged human or mouse GLP-1R or GIPR plasmids (Promega Corporation; Madison, WI). Cells were lifted using the TrypLE express enzyme (ThermoFisher Scientific) and plated at 80,000–100,000 cells per well in 96 well plates. Fourty 8 h later, media was replaced with assay buffer containing equal parts CO2 independent media and Nano-Glo HiBiT extracellular buffer containing LgBiT protein (1:100), and the Nano-Glo HiBiT extracellular substrate (1:50). Next, test compounds in DMSO were added to cells, and plates were read on an EnVision multimode plate reader (PerkinElmer; Waltham, MA), for 120 min at 2-min intervals.

Intraperitoneal glucose tolerance test

Liraglutide and CT-859 were administered by a single subcutaneous injection (SC) at the doses provided in each figure 4–48 h before the intraperitoneal glucose tolerance test (ipGTT). On the day of the ipGTT, mice were fasted for 5 h. Baseline blood glucose was determined using an AlphaTrakII glucose meter from whole blood collected from the tip of the tail. After that, glucose 2 g/kg dextrose (as a 20% solution in saline) was injected by a single intraperitoneal injection. Blood glucose was determined at the specified time intervals in each figure. When plasma insulin concentration was desired, mice were warmed under a heat lamp, blood glucose concentration was determined, and ~20μL whole blood was collected in K2-EDTA microvettes (Sarstedt). The area under the curve (AUC) analysis was performed using GraphPad Prism software with the baseline set at Y = 0.

Food consumption

Acute food intake

Mice were weighed, glucose levels were measured using a Nova Biomedical glucose meter (Data Sciences International), and treatments were administered by a single SC injection or an intracerebroventricular injection into the lateral ventricle. Mice were returned to their cage with a pre-weighed amount of food on the cage floor. Body weight, food consumption, and glucose levels were measured 24, 48, and up to 72 h post-treatment administration.

Intracerebroventricular cannulations

Male C57BL/6J and GLP-1RKO, wild type littermates were implanted with a 26-gauge guide cannula with a 5 mm pedestal, and the cannula cut 1.6 mm below the pedestal using the following coordinates: anterior-posterior (AP); −0.4 mm, R/L; 1 mm, dorsal-ventral (DV); −1.3 mm. Mice were allowed to recover for one week. After one week, mice were manually restrained and injected with vehicle or compounds using a 33-gauge internal cannula injector with a 0.8 mm projection.

Weight loss

DIO mice were acclimated to daily weighing and handling for approximately 1 week until their weight had stabilized. Mice were injected subcutaneously once daily with the indicated dose of peptide, or vehicle, based on current body weight. Injections were performed 6 h before the dark cycle started to approximate reaching T_{max} when the dark cycle started. Where indicated, 24-h food consumption studies were performed as described above. Body weight as a percentage of initial weight was calculated daily by dividing the daily body weight by the body weight taken before the first dose of peptide, multiplied by 100%. Blood glucose was determined at study termination, and blood was collected to quantify plasma insulin concentrations. Mice were sedated by isoflurane and euthanized by decapitation. Whole trunk blood was collected in K2-EDTA microvettes and was kept on ice until centrifugation at 5000 *rcf* for 10 min at 4°C. Plasma was stored at −80°C until analysis. Subcutaneous and inguinal fat and the liver were removed and weighed.

Caloric restriction

As indicated above, DIO mice were acclimated to daily weighing and handling for approximately 1 week until their weight had stabilized. Mice were randomized, into the following groups: vehicle, 60% caloric restriction (60% CR), and CT-859 (200 nmol/kg), based on body weight. Mice were injected subcutaneously once daily with the indicated dose of peptide, or vehicle, based on current body weight. The CR group received 40% of their average food consumption on a daily basis for 6 days. Results are presented as percentage of initial weight calculated as described above.

Pharmacokinetics

Pharmacokinetic (PK) analysis for CT-859 and liraglutide were performed in CD-1 male mice by BioDuro inc. For the PK analysis of CT-693 and CT-666, C57BL/6J male mice were injected with compounds by a single subcutaneous injection, and plasma was collected at 15, 30, 60, 120, and 240 min post compound administration. Plasma concentrations were quantified using an LC-MS API 7500 by MeadowHawk Biolabs.

Plasma insulin

Whole blood collected in K2-EDTA microvettes was kept on ice until centrifugation at 5000 *rcf* for 10 min at 4°C. Plasma was removed and stored at −80°C until analyzed. Plasma insulin concentrations were determined using the U-PLEX Mouse Insulin Assay (Meso Scale Discovery).

QUANTIFICATION AND STATISTICAL ANALYSIS

Results are presented as means (± standard error). We used an unpaired t-test to detect a difference between two groups. We used a one-way ANOVA with Bonferroni's test for multiple comparisons to detect a difference between more than two groups. For everything else, we used a two-way ANOVA with group and time as between-subject factors. Multiple comparisons were carried out using a Bonferroni correction. Nonlinear regression analysis with the Hillslope constrained to 1 was used to fit normalized *in vitro* data to a curve. Compound potency (EC_{50}) and efficacy (E_{max}) were extracted from this analysis. Statistical analyses were performed with GraphPad Prism 9.2.0 (GraphPad Software, Boston, MA). The number of samples in each graph is denoted in the figure legend. Statistical significance was set at $^{*}p < 0.05$, $^{**}p < 0.01$, $^{***}p < 0.001$, $^{****}p < 0.0001$, and letter $p < 0.05$.